Article

Dissociation of Carbanions from Acyl Iridium Compounds: An Experimental and Computational Investigation

Joseph G. Cordaro, and Robert G. Bergman

J. Am. Chem. Soc., **2004**, 126 (51), 16912-16929• DOI: 10.1021/ja045859l • Publication Date (Web): 07 December 2004

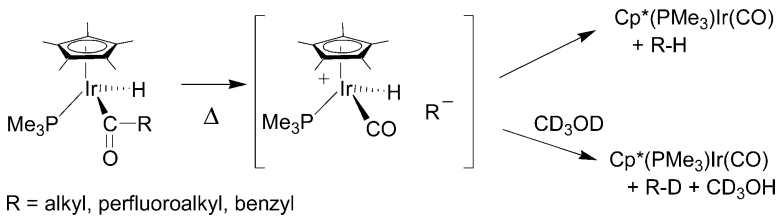

R = alkyl, perfluoroalkyl, benzyl

More About This Article

Additional resources and features associated with this article are available within the HTML version:

- Supporting Information
- Access to high resolution figures
- Links to articles and content related to this article
- Copyright permission to reproduce figures and/or text from this article

View the Full Text HTML

J|A|C|S
ARTICLES
Published on Web 12/07/2004

Dissociation of Carbanions from Acyl Iridium Compounds: An Experimental and Computational Investigation

Joseph G. Cordaro and Robert G. Bergman*

Contribution from the Department of Chemistry, University of California, Berkeley, California 94720

Received July 9, 2004; E-mail: bergman@cchem.berkeley.edu

Abstract: Instead of reductive elimination of aldehyde, or decarbonylation to give a trifluoroalkyl hydride, heating $Cp^*(PMe_3)Ir(H)[C(O)CF_3]$ (**1**) leads to the quantitative formation of $Cp^*(PMe_3)Ir(CO)$ (**2**) and CF_3H. Kinetic experiments, isotope labeling studies, solvent effect studies, and solvent-inclusive DFT calculations support a mechanism that involves initial dissociation of trifluoromethyl anion to give the transient ion-pair intermediate $[Cp^*(PMe_3)Ir(H)(CO)]^+[CF_3]^-$. Further evidence for the ability of CF_3^- to act as a leaving group came from the investigation of the analogous methyl and chloride derivatives $Cp^*(PMe_3)Ir(Me)[C(O)CF_3]$ and $Cp^*(PMe_3)Ir(Cl)[C(O)CF_3]$. Both of these compounds undergo a similar loss of trifluoromethyl anion, generating an iridium carbonyl cation and CF_3D in CD_3OD. Three additional acyl hydrides, $Cp^*(PMe_3)Ir(H)[C(O)R_F]$ (where $R_F = CF_2CF_3$, $CF_2CF_2CF_3$, or $CF_2(CF_2)_6CF_3$) undergo R_F-H elimination to give **2** at a faster rate than CF_3H elimination from **1**. Stereochemical studies using a chiral acyl hydride with a stereocenter at the β-position reveal that ionization of the carbanion occurs to form a tight ion-pair with high retention of configuration and enantiomeric purity upon proton transfer from iridium.

Introduction

The general interest in studying metal acyl complexes comes from their ubiquitous presence in stoichiometric and catalytic reactions involving carbon monoxide. For example, in the oxo reaction, CO and H_2 are added to olefins to produce aldehydes using catalytic cobalt or rhodium complexes. An important intermediate in this reaction is the metal acyl complex, which is cleaved either by a metal hydride or by H_2.[1] Many stoichiometric reactions, which introduce a carbonyl group into organic substrates, employ metal carbonyls and proceed via acyl intermediates. Isolable metal acyl complexes can be accessed by a wide range of methods, including oxidative addition of aldehydes or acid halides, insertion of CO into metal alkyl bonds, and nucleophilic addition to metal carbonyls.[2] Much of the reactivity of metal acyl complexes can be categorized into two broad areas: decarbonylation reactions and reductive elimination reactions.

Aldehyde decarbonylation using transition metal complexes requires a reactive species which oxidatively inserts into the C−H bond of an aldehyde. The newly formed metal acyl hydride species can undergo decarbonylation if a vacant coordination site is made available adjacent to the acyl group. Various techniques have been employed to produce an adjacent coordination site (e.g., ligand dissociation via photolysis or thermolysis, hydride abstraction).

Reductive elimination of aldehydes and ketones from metal complexes can occur upon thermolysis of acyl hydride or acyl alkyl complexes. Aldehydes have also been produced from alkyl carbonyl complexes upon treatment with a hydride source. Evidence for the intermediacy of an acyl complex has been obtained in many of these reactions. The rate of aldehyde reductive elimination from acyl hydrides is often very rapid and has been correlated to the metal−carbon bond strength.[3]

Because of the greater stability of metal perfluoroacyl and perfluoroalkyl complexes as compared to their all-hydrogen analogues, these complexes were among the earliest known organometallic species.[4] The stronger $M-CF_3$ bond as compared to $M-CH_3$ is partially responsible for the enhanced stability of the former toward thermal decomposition.[5−7] Routes for synthesizing metal perfluoroacyl complexes generally involve oxidative addition of a perfluoroacyl halide to a late transition metal carbonyl.[8,9] Rapid loss of CO followed by R_F migration (R_F = perfluoroalkyl) to generate the $(CO)M-R_F$ species can occur, often precluding the isolation of the metal acyl species. Isolation of the acyl $MC(O)R_F$ species can be achieved when a reactive open coordination site is not available at the metal center. Examples of CO inserting into a $M-R_F$ bond to give a perfluoroacyl complex are scarce.[10] Sulfur dioxide insertion into $M-R_F$ bonds has been observed;[11] however, due to the strong $M-R_F$ bond, perfluoroalkyl complexes are generally regarded as stable toward insertion reactions.[12]

(1) Collman, J. P.; Hegedus, L. S.; Norton, J. R.; Finke, R. G. *Principles and Applications of Organotransition Metal Chemistry*; University Science Books: Mill Valley, CA, 1987; Chapter 12.
(2) Crabtree, R. H. *The Organometallic Chemistry of the Transition Metals*; John Wiley & Sons: New York, 1994; Chapter 8.
(3) See ref 1, Chapter 5.
(4) Treichel, P. M.; Stone, F. G. A. *Adv. Organomet. Chem.* **1964**, *1*, 143−220.
(5) Morrison, J. A. *Adv. Inorg. Chem.* **1983**, *27*, 293−316.
(6) Brothers, P. J.; Roper, W. R. *Chem. Rev.* **1988**, *88*, 1293−1326.
(7) Morrison, J. A. *Adv. Organomet. Chem.* **1993**, *35*, 211−239.
(8) King, R. B.; Bisnette, M. B. *J. Organomet. Chem.* **1964**, *2*, 15−37.
(9) King, R. B. *Acc. Chem. Res.* **1970**, *3*, 417−427.
(10) Jablonski, C. R. *Inorg. Chem.* **1981**, *20*, 3940−3947.
(11) Von Werner, K.; Blank, H. *J. Organomet. Chem.* **1980**, *195*, C25−C28.

10.1021/ja045859l CCC: $27.50

Scheme 1. Thermolysis of **1** Gives CF_3H, Not Decarbonylation

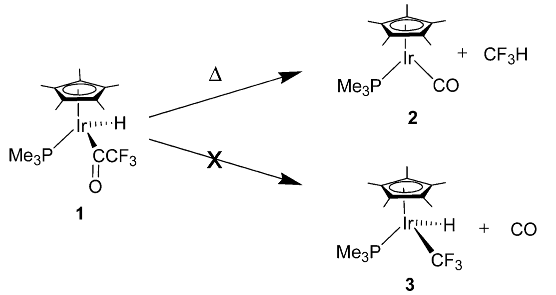

Perfluoroalkylmetal species are not as easy to synthesize using alkylation reactions of the type commonly used with their all-hydrogen cousins. The instability of perfluoroalkyllithium and -magnesium reagents toward fluoride elimination limits their use as perfluoroalkylating reagents.[13] Methods employing $Cd(CF_3)_2$ and $Hg(CF_3)_2$ to transfer trifluoromethyl to M−X species have been developed, but these routes are less popular due to safety and environmental concerns.[14−17] Oxidative addition of R_F−I to a metal can give a $M(I)R_F$ complex, but this method requires the initial formation of an unsaturated metal center.[18−20] More recently, Ruppert's reagent $CF_3Si(CH_3)_3$ has been successfully used to transfer CF_3 to both early and late transition metal halides.[21−23]

When we recently found that our new method for synthesizing iridium acyl hydrides[24] could be applied to the preparations of fluoroacyl complexes such as $Cp^*(PMe_3)Ir(H)[C(O)CF_3]$ (**1**, $Cp^* = \eta^5\text{-}C_5Me_5$), we were intrigued by the possibility of investigating such systems. Upon heating a C_6D_6 solution of **1** at 105 °C, we discovered that neither CO loss nor aldehyde reductive elimination occurred (Scheme 1). To our surprise, the products of this thermolysis reaction were CF_3H and the iridium(I) carbonyl $Cp^*(PMe_3)Ir(CO)$ (**2**).[25] The product of decarbonylation, $Cp^*(PMe_3)Ir(CF_3)H$ (**3**), was never observed. In this paper, we report our work on the mechanism of this unprecedented formal α-fluoroalkyl elimination reaction using both experimental and computational methods.

Experimental Results and Discussion

Synthesis of Acyl Complexes. The synthesis of **1** and the other acyl hydrides was accomplished using methods previously reported from this group (Scheme 2). Method 1[24] was preferred; treatment of $Cp^*(PMe_3)Ir(H)_2$ (**4**) with an acid chloride and base in benzene or toluene gave the desired acyl hydride complex in good yield. However, compound **5** was made by the reaction of $[Cp^*(PMe_3)IrHLi]_x$ with pentafluoropropanoic anhydride because the acid chloride was not readily available (method 2[26]). This method gives significantly lower yields due to the requirement for laborious purification. Two additional perfluoroacyl hydride complexes (**6** and **7**) were synthesized from the commercially available acid chlorides and **4** as shown in method 1. All solids were stored at −38 °C and showed no decomposition at this temperature. NMR (^{1}H, ^{19}F, ^{13}C, and ^{31}P) and IR spectroscopy and elemental analyses were used to characterize new compounds. (Crystallographic characterization of a related acyl hydride has been reported.[24]) All compounds exhibited broad doublets, due to P−H coupling, upfield in the ^{1}H NMR spectrum near −16 ppm characteristic of an iridium hydride. In the ^{31}P NMR spectrum, a signal near −38 ppm was observed for the PMe_3 ligand. Coupling of the phosphorus signal to the metal hydride was usually observed ($J_{H-P} \approx 30-40$ Hz). Solid or solution IR spectroscopy of the acyl hydrides showed a broad Ir−H stretch in the region 2110−2160 cm^{-1} and a strong carbonyl stretch near 1620 cm^{-1}.

Scheme 2. Two Methods for the Synthesis of Iridium Acyl Hydrides from **4**

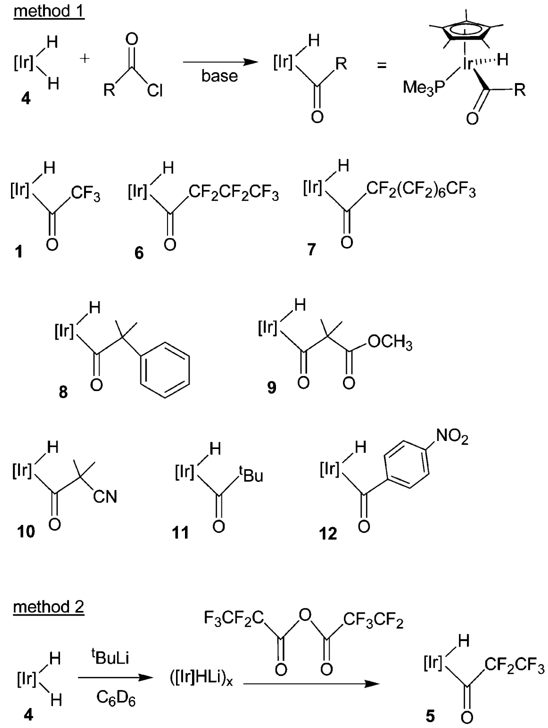

Five non-fluorine containing acyl hydrides were synthesized following method 1 and were used in this study. The phenyl-substituted acyl hydride **8** and methyl ester acyl hydride **9** were reported in the preliminary communication.[25] The cyanoacyl hydride **10** was synthesized in good yield and showed a characteristic C≡N stretch in the IR spectrum at 2225 cm^{-1} in addition to absorptions for the Ir−H and acyl C=O at 2095 and 1589 cm^{-1}, respectively. Methyl substituents at the β-position were used to prevent H_2O elimination, which has been observed to give a vinyl complex.[24] The 2,2-dimethylpropionyl (**11**) and *para*-nitrobenzoyl (**12**) hydrides were originally synthesized by Paisner et al.[24]

(12) Klabunde, K. J.; Campostrini, R. *J. Fluorine Chem.* **1989**, *42*, 93−104.
(13) For a recent review on the addition of a trifluoromethyl group to various organic compounds, see: Langlois, B. R.; Billard, T. *Synthesis* **2003**, 185−194.
(14) Lagow, R. J.; Eujen, R.; Gerchman, L. L.; Morrison, J. A. *J. Am. Chem. Soc.* **1978**, *100*, 1722−1726.
(15) Krause, L. J.; Morrison, J. A. *J. Am. Chem. Soc.* **1981**, *103*, 2995−3001.
(16) Dukat, W.; Naumann, D. *J. Chem. Soc., Dalton Trans.* **1989**, 739−744.
(17) Eujen, R.; Hoge, B. *J. Organomet. Chem.* **1995**, *503*, C51−C54.
(18) Clark, H. C.; Manzer, L. E. *J. Organomet. Chem.* **1973**, *59*, 411−428.
(19) Hughes, R. P.; Smith, J. M.; Liable-Sands, L. M.; Concolino, T. E.; Lam, K. C.; Incarvito, C.; Rheingold, A. L. *J. Chem. Soc., Dalton Trans.* **2000**, 873−879.
(20) Hughes, R. P.; Maddock, S. M.; Guzei, I. A.; Liable-Sands, L. M.; Rheingold, A. L. *J. Am. Chem. Soc.* **2001**, *123*, 3279−3288.
(21) Huang, D. J.; Koren, P. R.; Folting, K.; Davidson, E. R.; Caulton, K. G. *J. Am. Chem. Soc.* **2000**, *122*, 8916−8931.
(22) Vicente, J.; Gil-Rubio, J.; Bautista, D. *Inorg. Chem.* **2001**, *40*, 2636−2637.
(23) Taw, F. L.; Scott, B. L.; Kiplinger, J. L. *J. Am. Chem. Soc.* **2003**, *125*, 14712−14713.
(24) Paisner, S. N.; Burger, P.; Bergman, R. G. *Organometallics* **2000**, *19*, 2073−2083.
(25) Cordaro, J. G.; Bergman, R. G. *J. Am. Chem. Soc.* **2004**, *126*, 3432−3433.
(26) Peterson, T. H.; Golden, J. T.; Bergman, R. G. *Organometallics* **1999**, *18*, 2005−2020.

Scheme 3. Possible Mechanisms for the Loss of CF_3H from **1**

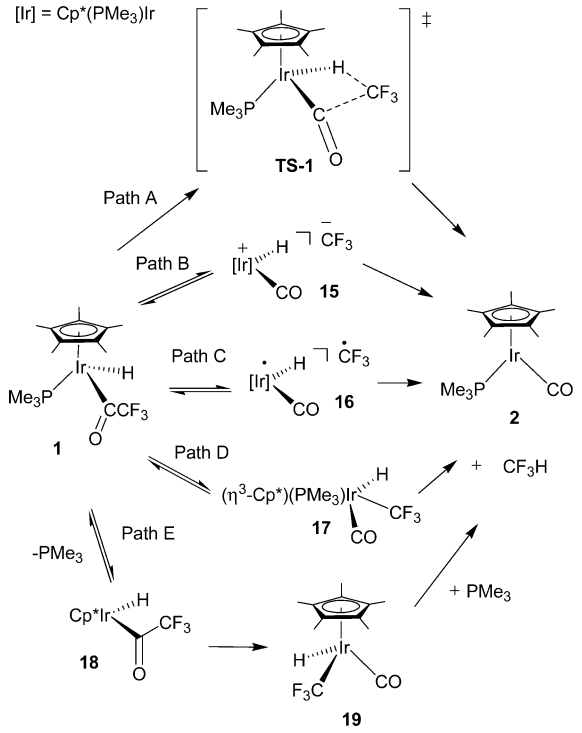

Two nonhydride iridium acyl compounds were synthesized from **1**. The methyl-substituted acyl complex **13** was synthesized by vacuum transfer of anhydrous THF into a Schlenk tube containing **1** and solid *tert*-butyllithium at −196 °C. The solution was warmed to −15 °C to ensure complete deprotonation of the metal hydride. Recooling the orange solution to −196 °C followed by vacuum transfer of iodomethane to this solution generated the alkylated product $Cp^*(PMe_3)Ir[C(O)CF_3](CH_3)$ (**13**) in 72% isolated yield (eq 1). The chloride-substituted acyl

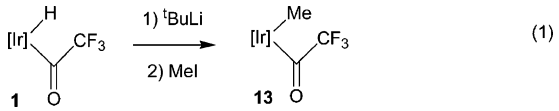

(1)

complex **14** was synthesized in approximately 83% yield by treating dihydride **4** and proton sponge (1,8-bis(dimethylamino)-naphthalene) with a 10-fold excess of trifluoroacetyl chloride (eq 2). Presumably, under these reaction conditions, **1** is initially formed but then chlorinated by excess acid chloride. Alternatively, **14** was synthesized by treating a solution of **1** in CD_2Cl_2 with CCl_4. Both **13** and **14** exhibited strong absorptions in the IR spectrum for the carbonyl group at 1619 and 1627 cm^{-1}, respectively.

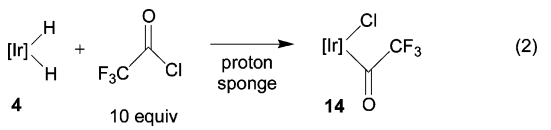

(2)

Mechanisms for Elimination of CF_3H from 1. Heating a C_6D_6 solution of **1** in a sealed NMR tube gave the iridium carbonyl **2** and CF_3H in quantitative yield. We considered seven mechanisms for this unusual transformation (Schemes 3 and 4).

Scheme 4. Possible Acid/Base-Catalyzed Mechanisms for the Loss of CF_3H from **1**

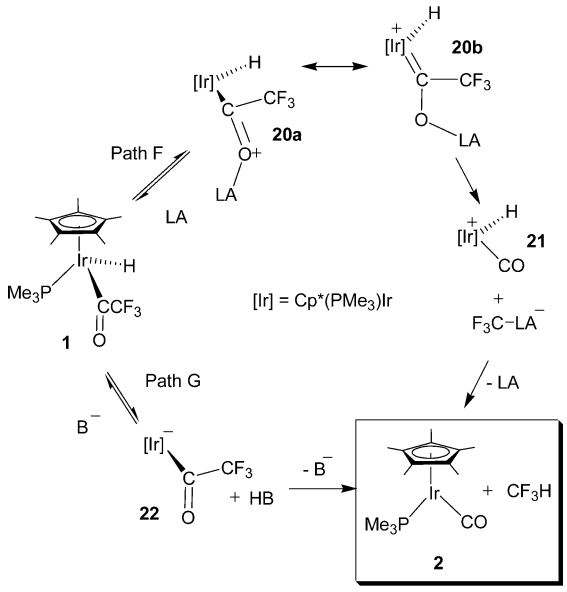

The first five mechanisms are intramolecular reactions (Scheme 3). Path A is a concerted, irreversible elimination of CF_3H from **1** via **TS-1** to generate the observed products. This proposed concerted α-fluoroalkyl elimination is unprecedented in organometallic chemistry. Path B, also unprecedented,[27] requires that the CF_3 fragment, functioning as a leaving group, reversibly dissociates to generate an intermediate metal cation/carbanion pair **15**. CF_3^- irreversibly deprotonates the iridium cation to generate the observed products. Alternatively, the reaction can be envisioned to proceed through a radical mechanism (Path C); reversible homolytic cleavage of the $C(O)-CF_3$ bond generates a metal acyl/fluoroalkyl radical pair **16**. The CF_3 radical then abstracts a hydrogen atom from iridium to generate the observed products. Path D illustrates a more common mechanism for the reactivity of metal acyl complexes: reversible migration of CF_3 to iridium, which occurs simultaneously with Cp* ring slippage to provide an open coordination site, produces intermediate **17**. This species then undergoes reductive elimination of CF_3H, concurrent with recoordination of the Cp* ligand, to generate the observed products. However, it seems likely that intermediate **17** would also dissociate CO to generate the iridium(III) species $Cp^*(PMe_3)IrH(CF_3)$ (**3**), which we do not observe. In the fifth possible mechanism, reversible PMe_3 dissociation from **1** generates **18**, a reactive 16-electron intermediate species with an open coordination site at iridium (path E). Decarbonylation to generate the iridium(III) carbonyl (**19**) would be facile. Reductive elimination of CF_3H, possibly induced by PMe_3 association, yields the observed products. CO dissociation could also occur upon binding PMe_3 to furnish the trifluoromethyl iridium(III) hydride **3**.

The remaining two proposed mechanisms involve a Lewis acid or base catalyst (Scheme 4). In path F, a Lewis acid (LA) reversibly coordinates to the metal acyl oxygen to give adduct **20**, which has resonance contributions from forms **20a** and **20b**. Elimination of CF_3-LA generates a stable iridium carbonyl

(27) A fluoroalkyl carbanion/metal cation pair has been reported in W and Mo chemistry. See: Hughes, R. P.; Maddock, S. M.; Guzei, I. A.; Liable-Sands, L. M.; Rheingold, A. L. *J. Am. Chem. Soc.* **2001**, *123*, 3279−3288.

Table 1. Temperature and Solvent Dependence of k_{obs} for the Elimination of CF_3 Anion from **1**

solvent	temp (°C)	k_{obs} (s^{-1}) ($\times 10^4$)	solvent	temp (°C)	k_{obs} (s^{-1}) ($\times 10^4$)
C_6D_6	94.5	0.0375 (±0.0025)	CD_3CN	94.3	7.18 (±0.4)
C_6D_6	104.9	0.089 (±0.004)	DMF-d_7	94.3	4.1 (±0.6)
C_6D_6	120.2	0.396 (±0.008)	DMSO-d_6	70	0.91 (±0.02[b])
C_6D_6	136	1.41 (±0.05)	DMSO-d_6	79.9	2.52 (±0.06)
C_6D_6[a]	136	1.39 (±0.01)	DMSO-d_6	85.5	4.1 (±0.6)
C_6D_6	142.2	2.29 (±0.11)	DMSO-d_6	90.8	7.02 (±0.44)
CD_3OD	80	3.2 (±0.1[b])	DMSO-d_6[a]	90.8	7.12 (±0.05)
CD_3OD	94.3	1.7 (±0.1[b])	DMSO-d_6[d]	90.8	6.2 (±0.4)
CD_3OD	104.9	2.2 (±0[b])	DMSO-d_6	94.3	10.6 (±1.7)
CD_3OD[c]	104.9	7.0 (±0[b])	DMSO-d_6	99.3	16.1 (±0.1[b])

[a] Reaction done with deuterium labeled **1**-d_1. [b] Error calculated for fit. [c] Done with added **13**. [d] Done with 1 equiv of $MgCl_2$.

cation **21** and the CF_3−LA adduct. Proton transfer from iridium cation **21** to the CF_3−LA adduct liberates LA and forms the observed products. The final possible mechanism that we propose is an elimination reaction catalyzed by a Brønsted base (path G). Deprotonation of the iridium metal hydride with base (either reversibly or irreversibly depending on the strength of the base) generates the reactive iridate species **22**. The anionic intermediate **22** eliminates CF_3^- to give the iridium carbonyl **2**. Proton transfer from the conjugate acid to CF_3^- yields CF_3H and the free base.

Rate Studies on the Elimination of CF_3H from 1. The rate of disappearance of **1** and the formation of **2** followed clean first-order kinetics for all temperatures and solvents monitored. The proposed first-order rate law for the conversion of **1** to **2** is shown in eq 3. The rate was found to be independent of initial concentrations of **1** and was not affected by the addition of 5 equiv of PMe_3; therefore, reversible PMe_3 dissociation before the rate-limiting step to give an open coordination site at iridium as in path E is ruled out (Scheme 3). This observation is

$$-\frac{d[\mathbf{1}]}{dt} = \frac{d[\mathbf{2}]}{dt} = k_{obs}[\mathbf{1}] \qquad (3)$$

consistent with other work from this group showing that PMe_3 dissociation from Cp*(PMe_3)Ir complexes is very slow.[28] While Lewis acid coordination to the oxygen of an acyl group has been shown to increase the rate of alkyl−carbonyl migratory insertion reactions,[29] we found no effect of such reagents on the rate of reaction. For example, the addition of 1 equiv of $MgCl_2$ had no effect on the rate of CF_3H loss from **1** when measured in DMSO-d_6 (studies investigating the effect of H^+ on the rate of anion dissociation from **13** are discussed below). Treatment of **1** with the stronger Lewis acid triphenylcarbenium tetrakis(pentafluorophenyl)borate resulted in hydride abstraction and decarbonylation to give the iridium trifluoromethyl carbonyl cation (**23**) (eq 4). No elimination products were observed.

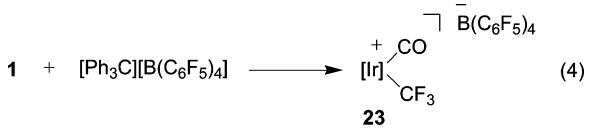

23 (4)

Solvent Effects. Solvent can play a critical role in the rate and product distribution of many organic and organometallic reactions. To investigate whether CF_3H loss from **1** was influenced by the medium, the rate of the reaction was measured using ^1H NMR spectroscopy in various solvents. We found that in polar aprotic solvents such as CD_3CN and DMSO-d_6 the rate of the reaction at 94 °C was accelerated approximately 200-fold compared to the rate in C_6D_6. Other solvents exhibited varying degrees of rate enhancement (Table 1).

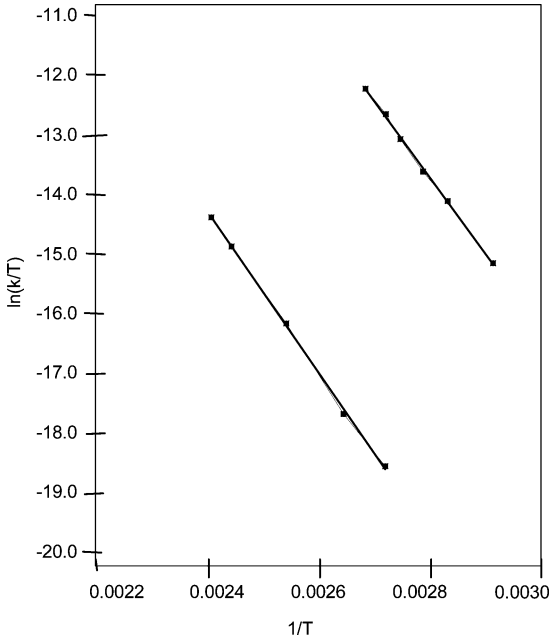

Figure 1. Eyring plots for the elimination of CF_3H from **1** in (a) C_6D_6 ($R^2 = 0.9991$) and (b) DMSO-d_6 ($R^2 = 0.9986$).

The activation parameters for the reaction in C_6D_6 and DMSO-d_6 were found to be: C_6D_6, $\Delta H^‡ = 25.7$ kcal/mol and $\Delta S^‡ = -14.0$ kcal/mol; DMSO-d_6, $\Delta H^‡ = 24.3$ kcal/mol and $\Delta S^‡ = -6.5$ kcal/mol. (See Figure 1 for Eyring plots.) The $\Delta\Delta G^‡$ between the two solvents is consistent with the observed rate difference.

The significant solvent effect on the rate of reaction was the first indication that the reaction might proceed through a polar transition state(s) and/or charged intermediate(s) (paths B, F, and G). Table 2 shows the correlations between rates in different solvents and various solvent parameters. While some trends can be observed, the best categorization of solvents screened appears to simply be nonpolar (benzene), dipolar protic (methanol), and aprotic dipolar solvents (CH_3CN, DFM, and DMSO), the latter group of solvents showing the largest effect on rate enhancement.

(28) Buchanan, J. M.; Stryker, J. M.; Bergman, R. G. *J. Am. Chem. Soc.* **1986**, *108*, 1537−1550.
(29) See ref 1, p 372.

Table 2. Correlation between Solvent Effect on Rate of Reaction and Solvent Parameters

Relative Rates of Reaction Measured at 94 °C:				
C_6D_6	< CD_3OD	< DMF-d_7	< CD_3CN	< DMSO-d_6
1	45	110	191	283
ϵ: Dielectric Constants of Solvents[a]				
C_6H_6	< CH_3OH	< DMF	< CH_3CN	< DMSO
2.28	32.7	36.7	37.5	46.68
μ: Dipole Moments of Solvents (debye)[a]				
C_6H_6	< CH_3OH	< CH_3CN	< DMF	< DMSO
0	2.87	3.44	3.86	3.90
$E_T(30)$: Electronic Transition Energies of Solvents (kcal mol^{-1})[b]				
C_6H_6	< DMF	< DMSO	< CH_3CN	< CH_3OH
34.3	43.2	45.1	45.6	55.4

[a] Lowry, T. H.; Richardson, K. S. *Mechanism and Theory in Organic Chemistry*; Harper Collins: New York, 1987. [b] Reichardt, C. *Chem. Rev.* **1994**, *94*, 2319−2358.

Isotope Effect and Isotope Tracer Studies. Rate studies using deuteride **1-d** showed no kinetic isotope effect (KIE) in either C_6D_6 or DMSO-d_6 (k_H/k_D = 1.01 in C_6D_6 and 0.994 in DMSO-d_6). This result necessitates that deprotonation of **1** is not rate-determining, as might be expected if path G wereoperative. Additionally, the negligible KIE suggests that reductive elimination of CF_3H from either of the proposed intermediates **17** or **19** is not rate-determining. The observation of an isotope effect is common in rate-determining reductive elimination reactions of late transition metal complexes.[28,30−33] The lack of a KIE is consistent with a mechanism involving CF_3 dissociation from **1** via an ionic or radical mechanism (paths B or C).

Further support for a mechanism involving initial dissociation of CF_3^- came from isotope tracer studies. When the reaction was carried out in CD_3OD, the product of the elimination reaction was not CF_3H, but CF_3D. Control experiments showed that (1) heating **1** in CD_3OD at temperatures lower than those required to form **2** did not incorporate D into the hydride position of **1** and (2) heating **2** and CF_3H in CD_3OD did not incorporate D into trifluoromethane. Using CH_3OD, only **2** and CF_3D were formed, confirming that the H(D) arose from the OH(OD) group of the methanol solvent. This result conclusively ruled out the possibility of a radical mechanism.[34] In CH_3OD, one would expect CF_3H to form only if $CF_3^\bullet$ were generated, because the trifluoromethyl radical would abstract a hydrogen from the weaker C−H bond (BDE = 96.1 ± 0.2 kcal/mol) in preference to the more strongly bound hydroxyl-deuterium atom (>104.6 ± 0.7 kcal/mol).[35] We conclude that deuterium incorporation into the trifluoromethane product occurs via an ionic mechanism (path B).

Thermolysis of **1** in DMSO-d_6, CD_3CN, THF-d_8, and DMF-d_7 provided more evidence for the formation of CF_3D via an ionic mechanism. In CD_3CN or DMSO-d_6, both CF_3H and CF_3D were generated in approximately 1:1.9 and 1:0.9 ratios. In THF-d_8 or DMF-d_7, only **2** and CF_3H were generated; no CF_3D was observed. The pK_a values and bond dissociation energies (BDE) of these solvents are consistent with the observed deuterium incorporation into the trifluoromethane product via protonolysis.

Table 3. Rate of Elimination for Acyl Compounds Other than **1**

compound	solvent	temp (°C)	k_{obs} (s^{-1}) (×10^4)
CF_3CF_2 **5**	C_6D_6	104.9	1.80 (±0.02)
$CF_3CF_2CF_2$ **6**	C_6D_6	104.9	14.9 (±0.6)
$CF_3(CF_2)_6CF_2$ **7**	C_6D_6	104.9	26 (±1)
dimethylbenzyl **8**	C_6D_6	135.8	0.147 (±0.003)
ester **9**	C_6D_6	135.8	0.043 (±0.002)
ester **9**	DMSO-d_6	135.8	4.9 (±0.1)
cyano **10**	tol-d_8	104.9	14.1 (±0.4)
methyl **13**	CD_3OD	104.9	30.1 (±0.4)
chloride **14**	CD_3OD	104.9	0.138 (±0.001)
chloride **14**	DMF-d_7	104.9	0.036 (±0.001)

The similar BDEs of DMSO-d_6 (BDE = 94 kcal/mol),[36] CD_3CN (BDE = 93 kcal/mol),[37] and THF-d_8 (BDE = 92−93)[38,39] indicate that a mixture of CF_3H and CF_3D would be formed in all three solvents if a radical mechanism was operative, not just in CD_3CN or DMSO-d_6. The acidities of the solvents, however, do coincide with protonation of CF_3^-. The pK_a of CF_3H has been estimated to be approximately 29 in DMSO[40] or 27 in water at 0 °C.[41] CF_3^- is probably not basic enough to deprotonate DMF or THF even at elevated temperatures. However, deprotonation of CH_3CN (pK_a = 26.5 in CH_3CN),[42] CH_3OH (pK_a = 17 in CH_3OH), or DMSO (pK_a = 35.1 in DMSO)[43] by CF_3^- at elevated temperatures would be possible.

Elimination of R−H from Other Acyl Hydrides. Three additional perfluoroalkyl hydride complexes (**5**−**7**) were found to undergo elimination of R_F−H upon heating. Significantly faster rate constants for elimination were measured for the complexes with longer perfluoroalkyl chains (Table 3). Whereas in C_6D_6 at 105 °C the half-life for CF_3H elimination from **1** was 21.6 h, the half-life for HCF_2CF_3 elimination from **5** was 1.1 h. The half-lives for elimination of $HCF_2CF_2CF_3$ from **6** and $HCF_2(CF_2)_6CF_3$ from **7** under the same conditions were only 7.8 and 4.5 min, respectively. Due to the volatile nature of the elimination product from **1**, the rate of reaction could not be accurately monitored by ^{1}H or ^{19}F NMR spectroscopies using the resonances for CF_3H. In contrast, measuring the rate of formation of $HCF_2CF_2CF_3$ from **6** and $HCF_2(CF_2)_6CF_3$ from **7** by ^{1}H NMR gave rate constants equivalent to the rate constants determined by monitoring the formation of **2** or the disappearance of starting materials. The yields of the longer perfluoroalkane products were >90% as determined by NMR integration. No fluoroalkenes, the product of fluoride elimination, were observed for the reactions in C_6D_6, but in polar solvents, elimination products were observed. These results provide further support for the intermediacy of perfluorocarbanions, which are stabilized inductively and live long enough in polar solvent to undergo some fluoride elimination.

Two nonfluoroacyl groups were shown to undergo carbanion dissociation, albeit at higher temperatures. Compound **8** under-

(30) Periana, R. A.; Bergman, R. G. *J. Am. Chem. Soc.* **1986**, *108*, 7332−7346.
(31) Churchill, D. G.; Janak, K. E.; Wittenberg, J. S.; Parkin, G. *J. Am. Chem. Soc.* **2003**, *125*, 1403−1420.
(32) Janak, K. E.; Parkin, G. *J. Am. Chem. Soc.* **2003**, *125*, 6889−6891.
(33) Jones, W. D. *Acc. Chem. Res.* **2003**, *36*, 140−146.
(34) For related experiments, see ref 27 and references therein.
(35) Blanksby, S. J.; Ellison, G. B. *Acc. Chem. Res.* **2003**, *36*, 255−263.
(36) Bordwell, F. G.; Liu, W. Z. *J. Phys. Org. Chem.* **1998**, *11*, 397−406.
(37) Bordwell, F. G.; Zhang, X. *J. Org. Chem.* **1990**, *55*, 6078−6079.
(38) Muedas, C. A.; Ferguson, R. R.; Brown, S. H.; Crabtree, R. H. *J. Am. Chem. Soc.* **1991**, *113*, 2233−2242.
(39) Laarhoven, L. J. J.; Mulder, P. *J. Phys. Chem. B* **1997**, *101*, 73−77.
(40) Andrieux, C. P.; Gelis, L.; Medebielle, M.; Pinson, J.; Saveant, J. M. *J. Am. Chem. Soc.* **1990**, *112*, 3509−3520.
(41) Symons, E. A.; Clermont, M. J. *J. Am. Chem. Soc.* **1981**, *103*, 3127−3130.
(42) Coetzee, J. F.; Padmanabhan, G. R. *J. Phys. Chem.* **1962**, *66*, 1708−1713.
(43) Matthews, W. S.; Bares, J. E.; Bartmess, J. E.; Bordwell, F. G.; Cornforth, F. J.; Drucker, G. E.; Margolin, Z.; McCallum, R. J.; McCollum, G. J.; Vanier, N. R. *J. Am. Chem. Soc.* **1975**, *97*, 7006−7014.

Scheme 5. Decomposition of **9** May Arise from Ketene Formation

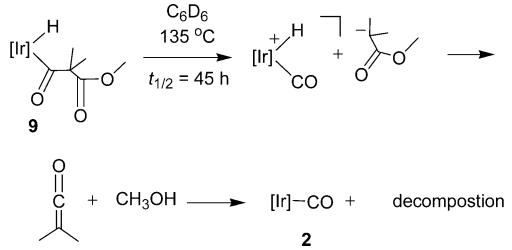

went elimination slowly as compared to **1** ($t_{1/2} = 13.3$ h at 136°C in C_6D_6), to give **2** and 2-phenylpropane (>95% yield, eq 5).

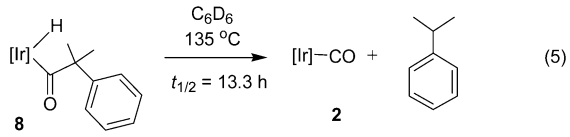

(5)

The elimination reaction of **8** in CD_3OD generated 2-deuterio-2-phenylpropane. The slow rate of elimination from the acyl hydride **8** is consistent with the inability of the dimethylbenzyl anion to efficiently stabilize a negative charge. Compound **9** decomposed to **2** in low yield and unidentifiable organic products at a considerably longer reaction time as compared to **1** (reaction time for **9**: $t_{1/2} = 24$ min at 135 °C in DMSO-d_6 and $t_{1/2} = 45$ h at 135 °C C_6D_6). The longer half-life measured for the elimination reaction from **9** was surprising. Furthermore, decomposition of the organic products, and eventually the iridium carbonyl **2**, at longer reaction times prevented further investigation. One possible explanation for the decomposition products is that, although **9** dissociates to the intermediate ion-pair, the resulting carbanion eliminates methoxide to form a ketene product (Scheme 5). At the high temperature required for dissociation, the resulting ketene product is expected to undergo decomposition.

In contrast to **1**, the 2,2-dimethylpropionyl (**11**) and para-nitrobenzoyl-(**12**) iridium compounds were unreactive upon heating in C_6D_6 or DMSO-d_6 below 135 °C; above this temperature, complete decomposition occurred (eq 6). The prohibitively high activation energy required to generate *tert*-butyl carbanion or phenyl anion explains the lack of reactivity of these complexes.

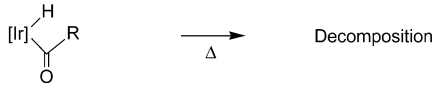

(6)

11 R = *tert*-butyl
12 R = *p*-nitrophenyl

Fluorenide anion has found utility in our group as a stable organic carbanion.[44] Substituted fluorenyl acyl iridium complexes appeared to be good candidates for investigating the effects of pK_a changes on the rate of anion dissociation. A wide range of pK_a values of substituted fluorenes are known; fluorene itself has a pK_a of 22.6 in DMSO.[43] Unfortunately, all attempts to synthesize the fluorenyl analogue (**24**) of the iridium acyl hydride under a variety of conditions were unsuccessful (Scheme 6). Treatment of iridium dihydride **4** and proton sponge with 9-fluorenonyl chloride (**25**) in C_6D_6, C_6D_{12}, or THF-d_8 resulted

Scheme 6. Reaction of Dihydride with Fluorenonyl Chlorides

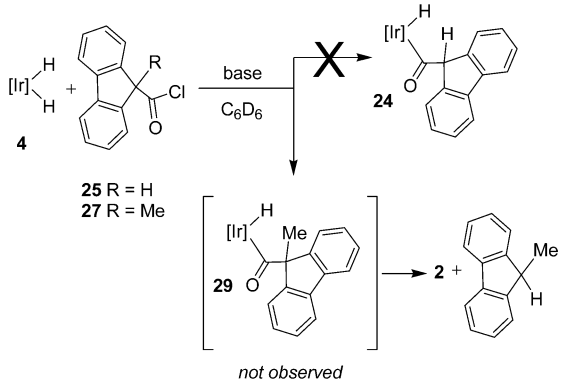

in the production of Cp*(PMe_3)$IrCl_2$ (**26**). We hypothesized that the β-hydrogen at the 9-position of the fluorene was undergoing deprotonation during the reaction to generate a ketene. To prevent this undesired transformation, 9-methyl-9-fluorenonyl chloride (**27**) was synthesized and reacted with dihydride **4** and proton sponge in C_6D_6. After 36 h at 25 °C, an equal amount of 9-methylfluorene and iridium carbonyl **2** in addition to unreacted starting materials with trace amounts of Cp*(PMe_3)IrHCl (**28**) were observed by NMR spectroscopy. None of the desired iridium acyl hydride (**29**) was detected. Replacement of the 9-hydrogen with a methyl group successfully blocked the decomposition pathways, but the rapid elimination of 9-methylfluorene prevented the isolation of **29**. These experiments suggest that the stability of the anion and pK_a are not the only important factors that control which acyl groups will undergo facile elimination.

Stabilization of the transition state for anion dissociation via an inductive effect was demonstrated for the thermolysis of compounds **1** and **5**−**9**. With increasingly longer perfluoroalkyl chains, the rate of anion elimination increased. For the nonperfluoroacyl compounds, stabilization of the transition state was predicted to occur via both resonance and inductive effects; the π-system of the phenyl substituent in **8** and the ester substituent in **9** was expected to facilitate anion dissociation by delocalization of the negative charge. Surprisingly, acyl complexes **8** and **9**, which should lead to phenyl- and carbonyl-stabilized anions, respectively, were very slow to undergo anion dissociation. In contrast, isolation of the fluorenyl-substituted acyl complex **29** was not possible due to rapid elimination which furnished **2** and 9-methylfluorene (see Scheme 6).

A reason for the slow rates of elimination from **8** and **9**, but rapid in situ elimination of 9-methylfluorene from **29**, may be the orientation of the π-system of the acyl substituents. Figure 2 illustrates possible low-energy conformations of **8** and **9**. In these conformations, the phenyl group in **8** and ester group in **9** lie in a "staggered" orientation that minimizes steric repulsion between these groups and the two methyl groups on the adjacent carbon. If this conformation is maintained as the C−carbonyl bond at the β-position cleaves, the sp^3 orbital in the breaking C−C bond is nearly orthogonal to the π-system of the aryl and ester substituents. This orientation will minimize orbital overlap and stabilization of the developing negative charge as the transition state is approached. In contrast, the arene π-system in **29** is locked into a conformation in which there is good overlap between the developing orbital in the cleaving bond and the fluorenyl π-system. This conformation would lead to

(44) Fulton, J. R.; Sklenak, S.; Bouwkamp, M. W.; Bergman, R. G. *J. Am. Chem. Soc.* **2002**, *124*, 4722−4737.

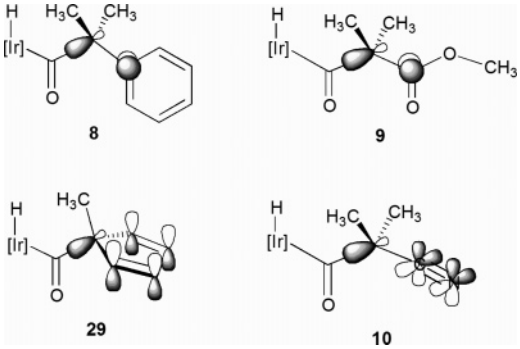

Figure 2. The dimethylmethylene linker inhibits rotation of the phenyl and ester substituents, so that in the lowest-energy conformations, the illustrated orbitals in **8** and **9** are orthogonal to one another. However, in compound **29**, the fluorenyl π-system overlaps well with the sp^3 bond being broken in **29** because of the structural rigidity of the system, and in **10** because of the cylindrical shape of the cyano substituent. (Eight carbon atoms of the fluorene substituent **29** have been omitted for clarity.)

rapid anion dissociation from **29** because of the better resonance stabilization of the negative charge.

To test this mechanistic hypothesis, we synthesized the cyano-substituted acyl hydride **10**. Because of the cylindrical symmetry of the π-system of the cyano group, its overlap with the developing orbital in the cleaving C−C bond should not be conformation-dependent. Therefore, our hypothesis predicts that the cyano substituent will stabilize the carbanion generated in the transition state no matter what its lowest-energy transition state conformation is.

Upon thermolysis of **10** in toluene-d_8 at 105 °C, **2** and 2-cyanopropane were generated in quantitative yield (eq 7). The

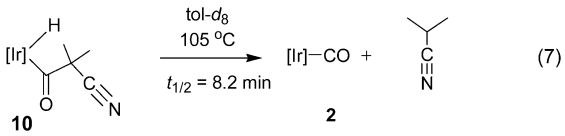

(7)

rate of elimination occurred with $t_{1/2} = 8.2$ min, hundreds of times faster than the rate of elimination from either **8** or **9** (Table 3).[45] This result supports our hypothesis that π-bond overlap is critical in stabilizing the transition state for anion dissociation.

Reaction of Cp*(PMe$_3$)Ir(H)[C(O)CF$_3$] with Base. To test the possibility of a base-catalyzed mechanism as illustrated in path G, Scheme 4, we treated **1** with both weak and strong bases. Thermolysis of **1** in C_6D_6 at 75 °C with 10 equiv of aniline or *n*-butylamine showed no catalytic reactivity for the elimination of CF_3H. The deprotonation of **1** with *tert*-butyllithium, however, was shown to occur at low temperature to give iridate **22-Li** (vide supra). Upon warming to 25 °C, iridate **22-Li** eliminated CF_3^- to give **2** and eliminated fluoride to give difluoroketene adduct **30** (Scheme 7).[46] No fluoride elimination was ever observed in the thermolysis of **1**. These results indicate that path G is operative in the presence of a strong base, where the reaction is fast even at low temperatures. It is unlikely, however, that the thermal reaction to generate **2** and CF_3H proceeds through intermediate **22**.

Stereochemical Studies of R−H Elimination. Next, we initiated a study of the stereochemistry of R−H elimination by

Scheme 7. Deprotonation of **1** with *tert*-Butyllithium Gives **2** and Difluoroketene **30**

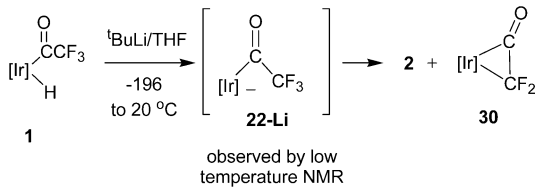

examining a β-chiral enantioenriched acyl hydride complex.[47] Upon synthesis of an iridium acyl hydride from an α-chiral acid chloride, a chiral center should be generated at the iridium center giving four enantiomers, two of which are diastereomers (Scheme 8). Elimination from this compound would give the achiral iridium carbonyl **2**, and an organic product with a tertiary carbon stereocenter. The enantiomeric excess (ee) of the organic product formed upon elimination would provide evidence about its mechanism. If elimination occurred through a concerted mechanism (path A), then the organic product would remain enantioenriched. If dissociation of R^- or $R^\bullet$ occurred to give a tight ion- or radical-pair, then R−H would remain enantioenriched, possibly with some loss of ee. However, if elimination gave solvent-separated ions or radicals, then the R−H product would be racemic. Migration of R to iridium followed by reductive elimination of R−H would likely occur with high overall retention of configuration. We decided to use enantioenriched Mosher's acid chloride (3,3,3-trifluoro-2-methoxy-2-phenylpropionyl chloride) to investigate the stereochemistry of the R−H elimination.

Reaction of 4 with Mosher's Acid Chloride Reagent. The reaction of Cp*(PMe$_3$)IrH$_2$ (**4**) and proton sponge with enantioenriched (*R*)- or (*S*)-Mosher's acid chloride (99% ee) (1:1:1 ratio) in C_6D_6 or CD_3CN did not give any observable acyl hydride **31a** or **31b**. After approximately 9 days at 25 °C, or 12 h at 75 °C in C_6D_6, the only iridium-containing materials identified by NMR spectroscopy were dihydride **4**, hydridochloride **28**, and carbonyl **2** in a 1:1:3 ratio with a trace amount of dichloride **26** (Scheme 9). In CD_3CN, complete consumption of the acid chloride occurred after approximately 20 h at 25 °C, or 2 h at 75 °C.[48] The iridium-containing products in CD_3CN identified by ^1H and ^{31}P NMR spectroscopy were a mixture of **4**, **28**, hydrido carbonyl cation **21**,[49] and an unidentified iridium hydride product in a ratio of 1.0:0.81:2.9:0.41. A small amount of dichloride **26** was detected in the ^{31}P NMR spectrum. No intermediate species were observed over the course of the reaction in either solvent.

The reaction in C_6D_6 generated two major organic products. These products were identified by NMR spectroscopy, GC/MS, and chiral GC as 3,3,3-trifluoro-2-methoxy-2-phenylpropionaldehyde (**32**), the aldehyde derivative of Mosher's acid, and 2,2,2-trifluoro-1-methoxyethylbenzene (**33**), the product of decarbonylation/reduction of Mosher's acid chloride. The ratio of the aldehyde to alkane in C_6D_6 was approximately 1:2.5 (similar

(45) A significant solvent effect on the rate of elimination is not expected upon substituting toluene for benzene.
(46) Cordaro, J. G.; van Halbeek, H.; Bergman, R. G. *Angew. Chem., Int. Ed.* **2004**, *43*, 6366−6369.
(47) For some early examples on the mechanism and stereochemistry of aldehyde and acid chloride decarbonylation, see: (a) Walborsky, H. M.; Allen, L. E. *J. Am. Chem. Soc.* **1971**, *93*, 5465−5468. (b) Stille, J. K.; Fries, R. W. *J. Am. Chem. Soc.* **1974**, *96*, 1514−1518. (c) Lau, K. S. Y.; Becker, Y.; Huang, F.; Baenziger, N.; Stille, J. K. *J. Am. Chem. Soc.* **1977**, *99*, 5664−5672.
(48) Monitoring the reaction after 70 h indicated no further changes in product ratios.
(49) The solubility of the ammonium chloride salt in acetonitrile accounts for the presence of the protonate iridium carbonyl **21**.

Scheme 8. Generation of Two Diastereomers upon Reaction of **4** with an α-Chiral Acid Chloride

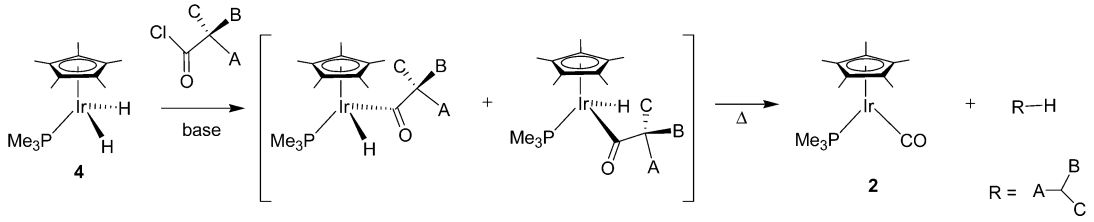

Scheme 9. Reaction of Dihydride **4** and Proton Sponge with Mosher's Acid Chloride

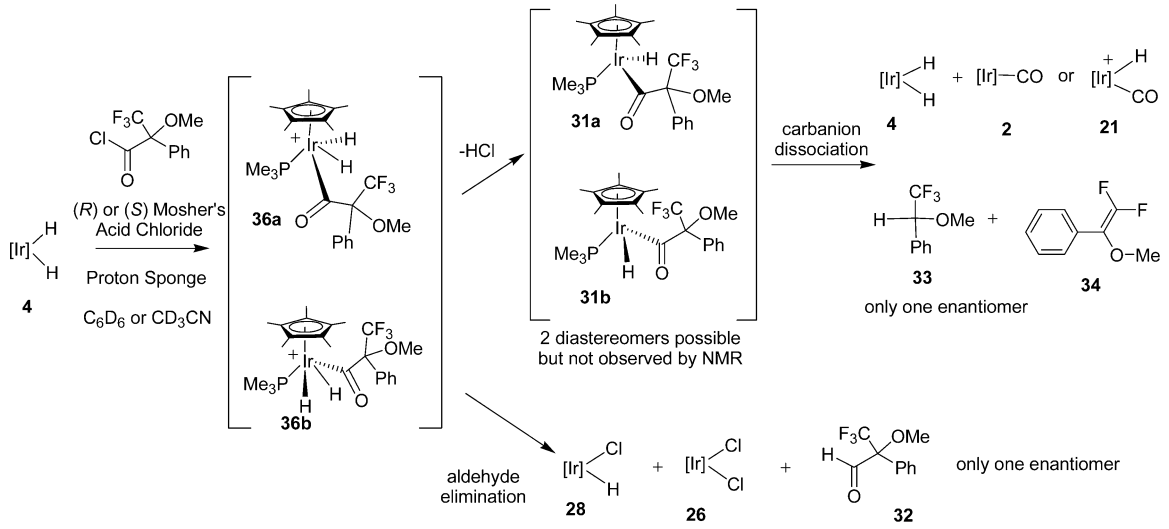

to the ratio of hydridochloride **28** to carbonyl **2**). Trace amounts of an alkene, identified as 1,1-difluoro-2-methoxy-2-phenylethene (**34**), were also observed in the ^{19}F NMR spectrum (Scheme 9). The ee values of the aldehyde **32** and alkane **33** determined by chiral GC were >98% and >96%, respectively.[50]

In CD_3CN, three major products were identified as aldehyde **32**, alkane **33**, and alkene **34** present in approximately a 1:1:1 ratio. Two unidentified fluorine-containing products (ca. 40% by integration) were detected. Using chiral GC, the ee was measured to be approximately 98% for the aldehyde and >96% for the alkane.

In the absence of proton sponge, the reaction of dihydride **4** with Mosher's acid chloride in C_6D_6 or CD_3CN gave the iridium hydrido carbonyl cation **21** rather than the carbonyl **2**. Two unidentified iridium-containing products were also observed. More of the iridium dichloride **26** was observed than when base was added, suggesting that free HCl was responsible for chlorination. Aldehyde **32**, alkane **33**, and alkene **34** were also formed in ratios similar to those observed in the reactions with added base. The ee's of the aldehyde and alkane as determined by chiral GC were high in both solvents (>97%).

In an alternative route to **31a**/**31b**, dihydride **4** was deprotonated with *tert*-butyllithium to generate $[Cp^*(PMe_3)IrHLi]_x$ and was subsequently treated with (*S*,*S*)-Mosher's anhydride in C_6D_6 at 25 °C. The only organometallic product identified by NMR spectroscopy was the iridium carbonyl **2** (eq 8). Analysis

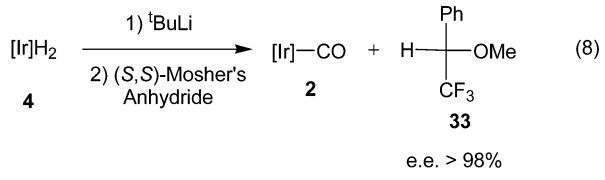

(8)

of the volatile materials by ^{1}H and ^{19}F NMR spectroscopy and chiral GC showed that the major product was alkane **33**, generated in >98% ee along with minor amounts of alkene **34**. This sequence of reactions, similar to method 2 (Scheme 2) for synthesizing acyl hydrides, confirms that acyl hydride **31a**/**31b** is a likely intermediate that quickly eliminates alkane **33** with high ee in the reactions depicted in both Scheme 9 and eq 8.

(*S*)-Aldehyde **32** was independently synthesized in >95% ee and 98% yield (by chiral GC) from (*S*)-Mosher's acid chloride and tributyltin hydride in C_6D_6 at 25 °C (Scheme 10).[51] The reaction of alkyl tin hydrides with acid chlorides was originally proposed to occur through a radical chain mechanism,[52] but later work showed that this reduction did not involve a radical chain process.[51]

To ensure that the radical (Ph)(MeO)(CF_3)C•, if formed, would be configurationally unstable and gave stereorandomized products, alkane **33** was generated via a radical mechanism using the method pioneered by Barton and co-workers (Scheme 10).[53] Metathesis of the thallium *N*-hydroxypyridine-2-thione salt[54] with (*R*)-Mosher's acid chloride furnished the pyridine thioether derivative **35** after radical-decarboxylative rearrangement. Thioether **35** was shown to be racemic (ca. 6.5% ee by chiral HPLC).[55] Photolysis of **35** in C_6D_6 in the presence of 9,10-

(50) In THF-d_8, the reaction was slightly faster than in C_6D_6 and gave rise to more alkene **34**.
(51) Lusztyk, J.; Lusztyk, E.; Maillard, B.; Ingold, K. U. *J. Am. Chem. Soc.* **1984**, *106*, 2923−2931.
(52) Kuivila, H. G.; Walsh, E. J. *J. Am. Chem. Soc.* **1966**, *88*, 571−576.
(53) Barton, D. H. R.; Crich, D.; Motherwell, W. B. *Tetrahedron* **1985**, *41*, 3901−3924.
(54) Aveline, B. M.; Kochevar, I. E.; Redmond, R. W. *J. Am. Chem. Soc.* **1995**, *117*, 9699−9708.
(55) Isolated crystals of thioether **35** showed no optical rotation, and analysis by chiral HPLC revealed that **35** consisted of a 1:1 ratio of enantiomers. Chiral HPLC of the crude reaction mixture containing **35** showed that the product was nearly racemic (9% ee).

Scheme 10. Independent Synthesis of Aldehyde **32** and Alkane **33** from Mosher's Acid Chloride

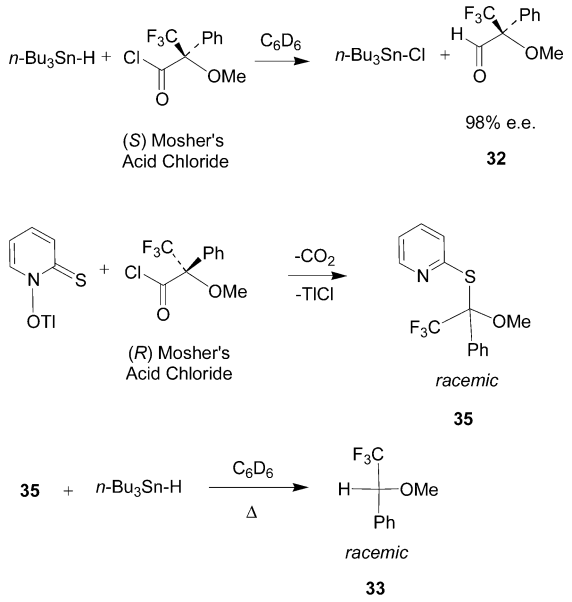

dihydroanthracene (DHA) gave a mixture of fluorine-containing products, including alkane **33**. Alternatively, thermolysis of **35** with 12 equiv of tributyltin hydride at 75 °C in C_6D_6 gave **33** in >95% yield by NMR. Analysis of the volatile materials by chiral GC confirmed that alkane **33** was racemic. These experiments show that the formation of $(Ph)(MeO)(CF_3)C^{\bullet}$ from an enantioenriched precursor leads to racemized products and rule out the intervention of this radical in the elimination from **31a**/**31b**.

In the reaction of Mosher's acid chloride with $Cp^*(PMe_3)IrH_2$ and proton sponge, the rate-limiting step is most likely initial nucleophilic attack at the carbonyl carbon of the acid chloride by the iridium metal center of the dihydride **4**.[24] This step is slow due to the steric bulk of the acid chloride; however, it appears to be faster in acetonitrile than in benzene (oxidative addition of RC(O)Cl to $Rh(CO)L_3Cl$ was reported to be much faster in acetonitrile than in benzene or toluene[56]). Rapid deprotonation of the resulting iridium cation **36** by proton sponge generates the acyl hydride product **31**. This complex, however, is unstable and undergoes elimination to generate alkane **33** and carbonyl complex **2**. The fast rate of elimination from **31a**/**31b** is likely due to inductive stabilization of the carbanion and possibly hyperconjugation from the trifluoromethyl substituent. The high enantioselectivity of alkane formation indicates a tight ion-pair intermediate which transfers a proton to the carbanion to give the observed products. In polar solvents, fluoride elimination to give alkene **34** occurs from the carbanion at a rate which is competitive with proton transfer. The ion-pair must react to give alkane **33** much more rapidly than the ions separate, because the ee of **33** is high in both solvents. Aldehyde **32** and hydridochloride **28** likely form by aldehyde reductive elimination from the acyl iridium dihydride cation **36** (Scheme 9).

Elimination of CF_3^- from 13 and 14. The reactivity of the trifluoroacyl group has provided strong support for the loss of CF_3H from **1** via an ion-pair mechanism (path B). Additional experiments have focused on the leaving group ability of the carbanion (e.g., CF_3, alkyl, or aryl). The importance of the hydride ligand and metal cation for CF_3^- loss from **1** has not been investigated. Therefore, to examine the role that might be played by the hydride ligand in the reactivity of compounds such as **1**, substituted trifluoroacyl iridium complexes with CH_3 (**13**) and Cl (**14**) in place of H were synthesized (vide supra).

Scheme 11. Possible Mechanisms for the Formation of Hydrido Iridium Carbonyl Cation from **14** in CH_3OH

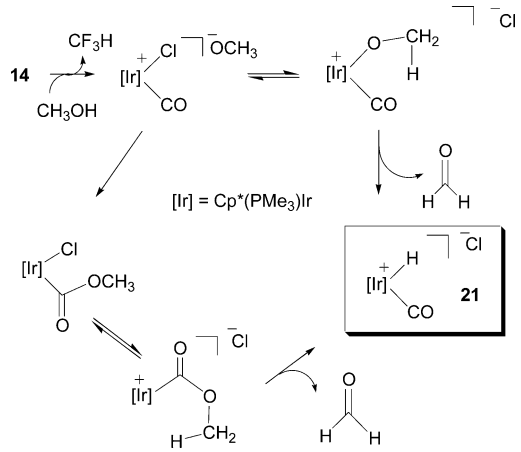

It was found that heating a CD_3OD solution of the acyl methyl compound **13** (eq 9) or acyl chloride compound **14** (eq 10) at 105 °C gave CF_3D and an iridium cation product in quantitative yield. In aprotic solvents (e.g., C_6D_6 or DMF-d_7), complete decomposition was observed. Formation of 1,1,1-trifluoroethane or trifluoromethyl chloride was not seen. The methyl acyl compound **13** underwent dissociation to give $Cp^*(PMe_3)Ir(CO)(CH_3)^+$ (**37**) and CF_3^-, and the latter reacted with CD_3OD to give CF_3D and methoxide-d_3 as the counterion. Upon thermolysis of **14**, the chloro carbonyl cation was not observed. NMR

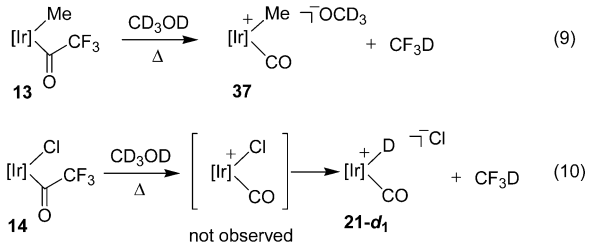

and IR analysis of the material isolated from this thermolysis reaction in protiated methanol revealed that the product was the hydrido iridium carbonyl cation **21**. This compound was independently synthesized by the method described by Angelici et al.[57] The chloro iridium carbonyl cation intermediate is most likely formed in situ. Two mechanisms for the transformation of the chloro cation in the presence of methoxide to **21** are proposed (Scheme 11). Both mechanisms involve displacement of chloride, hydride elimination, and liberation of formaldehyde.

In CD_3OD, the rate of disappearance of **13** to give the methyl cation followed first-order kinetics with a rate approximately 4 times faster than the rate for the conversion of **1** to **2** (Table 3). The disappearance of the chloro acyl complex **14** was found to be 51 times slower than the disappearance of **1** under identical conditions. CF_3^- dissociation is, not surprisingly, faster for the more electron-donating methyl compound **13** as compared to the chloro complex **14**. The methyl ligand is expected to stabilize

(56) Stille, J. K.; Fries, R. W. *J. Am. Chem. Soc.* **1974**, *96*, 1514−1518.

(57) Wang, D. M.; Angelici, R. J. *Inorg. Chem.* **1996**, *35*, 1321−1331.

Scheme 12. CF_3 Migration to Iridium Would Result in CO Dissociation

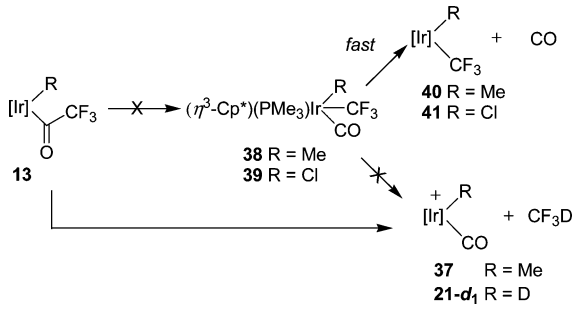

the resulting metal cation and possibly lower the activation energy. Conversely, the more electron-withdrawing chloro ligand destabilizes the iridium cation upon CF_3^- dissociation, resulting in a slower rate of reaction.

The results of hydride substitution with methyl- or chloro-ligands strongly disfavor both of the migration mechanisms (paths D or E in Scheme 2). Had migration of CF_3 to iridium occurred to give intermediate **38** (R = Me) or **39** (R = Cl), then rapid CO loss would be expected to give $Cp^*(PMe_3)Ir(CF_3)(R)$ (**40**, R = Me, or **41**, R = Cl). Reductive elimination of CF_3-R from these intermediates or protonolysis from CD_3OD solvent to give CF_3D and the observed products would be unlikely (Scheme 12).

Kinetic Studies on the Methyl Acyl Iridium Complex 13. Without the hydride attached to the metal center, as in the methyl acyl complex **13**, ionization of the CF_3 group can be studied directly. Proposed elementary steps for the dissociation of CF_3^- from methyl acyl complex **13** are illustrated in eqs 11 and 12. The first step, dissociation of CF_3^-, is potentially reversible. The second step, protonation of CF_3^- with an external acid (HA), is considered irreversible due to the high pK_a of CF_3H ($pK_a \approx 29$ in DMSO),[40] as long as HA is a substantially stronger acid. Using the steady-state approximation for the concentration of CF_3^-, a rate expression for d[**13**]/dt was derived (eqs 13 and 14).

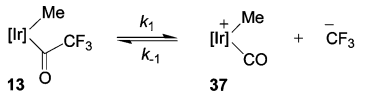

(11)

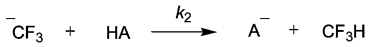

(12)

$$-\frac{d[\mathbf{13}]}{dt} = \frac{k_1k_2[\mathbf{13}][HA]}{k_{-1}[\mathbf{37}] + k_2[HA]} \quad (13)$$

$$-\frac{d[\mathbf{13}]}{dt} = \frac{k_1k_2[HA]}{k_{-1}[\mathbf{37}] + k_2[HA]}[\mathbf{13}] = k_{obs}[\mathbf{13}] \quad (14)$$

This rate expression predicts that, in the presence of excess HA and **37**, the rate should exhibit pseudo first-order kinetics, with a dependence of k_{obs} on both the concentration of **37** and HA. In principle, the value of k_{obs} should depend on the concentration of HA at low [HA] and high [**37**]; that is, inhibition by **37** and saturation in HA should both be observed. In practice, we found that when the rate of protonation was too slow, for example with high pK_a acids such as fluorene and 9-phenylfluorene, we observed complicated product mixtures and irreproducible rates (entries 1−4, Table 4). We believe this is due to the known decomposition of CF_3^- to fluoride ion and the reactive carbene CF_2.

Table 4. Rate Constants for the Disappearance of $Cp^*(PMe_3)Ir(Me)[C(O)CF_3]$ (**13**) in DMF-d_7 at 98 °C with Added Acid (HA) and $Cp^*(PMe_3)Ir(Me)(CO)^+$ (**37**)[a]

entry	13	37	HA	[HA]/[**37**]	k_{obs} (s^{-1}) ($\times 10^4$)
1	0.015[b]	0	0	NA	19[c]
2	0.015[b]	0.000	0.059[b,d]	NA	27[c]
3	0.015[b]	0.000	0.11[b,d]	NA	30[c]
4	0.015[b]	0.000	0.23[b,d]	NA	32[c]
5	0.014	0.036	0.069[d]	1.9	15
6	0.017	0.0	0.060[e]	NA	23[f]
7	0.015	0.140	0.046[e]	0.33	28
8	0.013	0.086	0.043[e]	0.53	29
9	0.043	0.130	0.14[e]	1.1	29
10	0.028	0.095	0.18[e]	2.0	34
11	0.014	0.050	0.19[e]	3.8	40
12	0.014	0.087	0.045[g]	0.52	21
13	0.015	0.054	0.20[g]	3.7	23
14	0.018	0	excess	NA	17 (±3)[h]

[a] Concentrations given in mol/L. [b] Concentration is approximate. [c] Initial rate data only. [d] Used 9-phenyl fluorine as HA. [e] Done with NMe_3HCl. [f] Rate of disappearance was equal to rate of product growth. [g] Done with 94% NMe_3DCl. [h] Average of five runs using a ratio of NMe_3HCl/NMe_3DCl between 1.3 and 0.0.

A stronger acid, therefore, was selected to react with CF_3^- and reduce the amount of decomposition. When 3.5 equiv of Me_3NHCl was added, clean first-order kinetics were seen for the entire reaction profile even in the absence of added **37** (entry 6, Table 4). The rate of starting material disappearance was equal to the growth of product ($-$d[**13**]/dt = d[**37**]dt), conditions not achieved when using 9-phenylfluorene as HA. Having found an acid that appeared to prevent CF_3^- decomposition, the ratio of [HA]/[**37**] was varied to look for product inhibition (entries 7−13, Table 4). Initial concentrations of starting acyl complex **13** were varied between 0.013 and 0.043 M. Concentrations of product **37** were varied between 0 and 0.14 M, and the concentrations of HA were varied between 0.045 and 0.20 M. Two runs using Me_3NDCl as HA showed a slight, but probably insignificant, decrease in k_{obs} (entries 12 and 13). A modest increase in k_{obs} with the highest ratios of [HA]/[**37**] (entries 10 and 11) as compared to k_{obs} for the lowest ratios of [HA]/[**37**] (entries 7, 8, and 12) was recorded. Overall, variations in the measured k_{obs} values were too minor to conclude that product inhibition was observed when Me_3NHCl was used as the acid. These results suggest that, under these conditions, fast protonation by HA ensured that $k_2[HA] \gg k_{-1}[\mathbf{37}]$. The HA term dominates the denominator of eq 14, reducing the rate law to the simple first-order expression in eq 15.

$$-\frac{d[\mathbf{13}]}{dt} = k_1[\mathbf{13}] \quad (15)$$

It is possible that addition of Me_3NHCl resulted in protonation of iridium or the acyl oxygen prior to CF_3^- dissociation, changing the mechanism to a Lewis acid-catalyzed reaction (similar to path F, Scheme 4). However, the measured k_{obs} with no added HA (entry 1) is similar to k_{obs} with added NMe_3HCl, suggesting that H^+ is not acting as a catalyst. Furthermore, in experiments using mixtures of Me_3NH/DCl (in excess relative to **13**), the ratio of CF_3H to CF_3D was approximately equal to the initial ratio of H^+/D^+ (entry 14, Table 4). No anomalous deuterium incorporation was observed, confirming that a preequilibrium, in which a proton coordinates to **13**, is not occurring.

Reactivity of $Cp^*(PMe_3)IrH(CF_2CF_2CF_3)$ (42) with CO. To test the possibility of fast and reversible CO dissociation

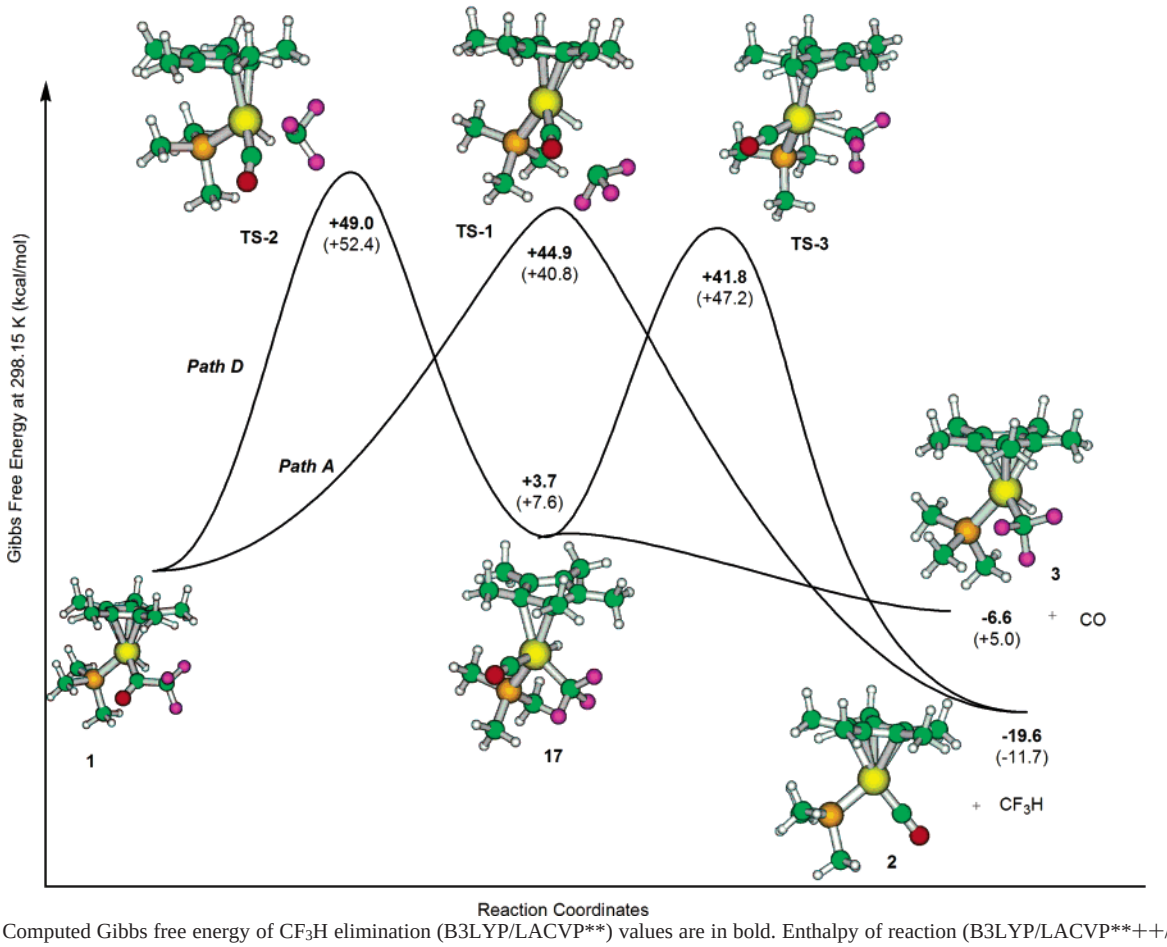

Figure 3. Computed Gibbs free energy of CF_3H elimination (B3LYP/LACVP**) values are in bold. Enthalpy of reaction (B3LYP/LACVP**++//B3LYP/LACVP**) values are in parentheses.

from intermediate **17** to give **3** versus R_F-H reductive elimination to give **2** (eq 16), we synthesized the perfluoroalkyl hydride complex Cp*(PMe_3)IrH($CF_2CF_2CF_3$) (**42**)[58] and treated it with CO. (Attempts to make **3** were not successful.) Heating a DMF-

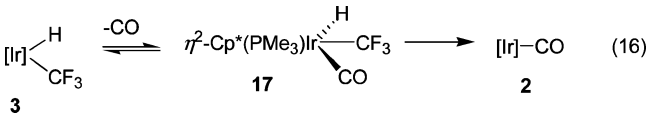

3 17 2 (16)

d_7 solution of **42** under an atmosphere of CO at 75 °C gave no iridium carbonyl **2** after 20 min (eq 17). In comparison, acyl hydride **6** eliminated $HCF_2CF_2CF_3$ to give **2** in <20 min at the same temperature. In C_6D_6, similar results were observed. While this result eliminates the possibility of fast and reversible CO dissociation from intermediate **17**, it does not preclude this species as an intermediate if CO dissociation is slow. Computational studies were therefore used to further elucidate the mechanism of CF_3H elimination from **1** and investigate the nature of a ring-slipped intermediate like **17**.

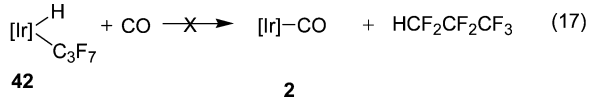

42 2 (17)

Computational Results and Discussion

Loss of CF_3H from 1: Gas-Phase Calculations. The geometries, energies, vibrational frequencies, and natural bond orders (NBO) of reactants, products, and possible intermediates and transition states for two of the mechanisms depicted in Scheme 3 were calculated using B3LYP density functional theory (DFT). Calculations for the loss of CF_3H from **1** focused on (1) the concerted elimination illustrated in path A and (2) migration of CF_3 to iridium followed by reductive elimination illustrated in path D, because experimentally these two mechanisms were the most difficult to distinguish.

Thermodynamically, the conversion of **1** to CF_3H and iridium carbonyl **2** was calculated to be more exergonic (ΔG(298.15 K) = −19.6 kcal/mol) than was the conversion of **1** to CO and iridium trifluoromethyl hydride **3** (ΔG(298.15 K) = −6.6 kcal/mol) (Figure 3). Entropy and zero-point-energy (ZPE) factors contribute approximately −9 kcal/mol to ΔG for the loss of either CO or CF_3H. The energies of all calculated species relative to **1** are given in Table 5.

Table 5. Calculated Energies (kcal/mol) Relative to **1**: Gas-Phase and Solution-Phase Calculations

compound	SCF energy[a]	Gibb's free energy[b]	single-point[c]	CH_3OH SCF energy[a]	CH_3OH single-point[c]	C_6D_6 SCF energy[a]	C_6D_6 single-point[c]	E_{solv} CH_3OH (kcal/mol)	E_{solv} C_6H_6 (kcal/mol)
1	0	0	0	0	0	0	0	−10.9	−4.2
2 + CF_3H	−5.4	−19.6	−11.7	−11.0	−13.8	−6.3	−13.1	−9.0	−3.7
3 + CO	9.1	−6.6	5.0	9.8	6.7	10.4	6.4	−9.0	−2.6
17	8.1	3.7	7.6	9.7	9.4	8.0	7.5	−9.1	−4.2
TS-1	49.5	44.9	40.8	35.6	21.3	44.3	32.5	−30.4	−12.5
TS-2	54.4	49.0	52.4	56.7	53.2	55.9	52.3	−10.1	−4.2
TS-3	47.0	41.8	47.2	49.8	50.4	46.9	47.2	−7.7	−4.2

[a] Geometry optimization done at the DFT B3LYP/LACVP** level. [b] Gibb's free energy calculated at 298.15 K and 1 atm. [c] Single-point calculations repeated using LACVP**++ basis set.

Table 6. Selected Bond Length (Å) Changes for CF_3H Loss via Two Calculated Mechanisms

	bond distance (Å)											
structure	Ir–H	Ir–(CO)	Ir–(PMe_3)	C–O	C(O)–CF_3	Ir–C(4)	Ir–C(5)	Ir–C(12)	Ir–C(10)	Ir–C(8)	H–(CF_3)	Ir–(CF_3)
1	1.596	2.010	2.286	1.227	1.568	2.316	2.318	2.386	2.357	2.338	3.122	NA
TS-1	1.578	1.890	2.343	1.155	2.884	2.301	2.276	2.471	2.440	2.285	2.249	NA
2	NA	1.834	2.274	1.173	NA	2.356	2.286	2.340	2.394	2.370	NA	NA
TS-2	1.591	1.870	2.248	1.176	2.033	3.409	3.083	2.968	2.322	2.358	3.005	2.723
17	1.623	1.947	2.334	1.154	NA	3.419	2.987	3.064	2.378	2.250	2.557	2.066
TS-3	1.736	1.854	2.319	1.183	3.661	3.303	3.037	2.779	2.246	2.291	1.401	2.367
3	1.588	NA	2.294	NA	NA	2.324	2.261	2.366	2.376	2.328	NA	2.042

A transition state (**TS-1**) located for the direct conversion of **1** to **2** was found to be 44.9 kcal/mol above **1**. It is clear that $\Delta G^{\ddagger}$ for this process is prohibitively high for a normal, solution-phase thermal organometallic reaction. However, upon further analysis, it becomes evident that the energy of **TS-1** is not unreasonable for this gas-phase calculation. The calculated geometric differences between **1** and **TS-1** are minimal except for the elongation of the acyl C−CF_3 bond length (see Table 6 for selected bond lengths). Calculations predicted the C−CF_3 bond length of the acyl group to increase from 1.568 to 2.884 Å, while there was negligible change (0.018 Å) in the Ir−H bond length upon going from **1** to **TS-1**. Most important to the energy of **TS-1** is the change in charge distribution. Results of NBO analysis showed that the calculated negative charge on the CF_3 group in **TS-1** increased from −0.09 in **1** to −0.769. The large negative charge on the CF_3 fragment suggests that **TS-1** more closely resembles a metal cation/carbanion pair, and the calculated high activation energy is, therefore, not unreasonable for a gas-phase heterolytic bond cleavage process.

An alternative mechanism, involving CF_3 migration to iridium followed by CF_3H reductive elimination, was also calculated (path D, Scheme 3). The transition state (**TS-2**) connecting **1** and intermediate **17** was found to be 49.0 kcal/mol in energy above **1** (Figure 3). Simultaneous with CF_3 migration to iridium in **TS-2** was a pronounced η^5- to η^2-ring slip of the Cp* ligand (Table 6). The unusual η^2- rather than η^3-coordination of the Cp* ligand was evident both geometrically and electronically. In **17**, the geometry at iridium was best described as trigonal bipyramidal with the hydride and CO ligands axial and the PMe_3, CF_3, and η^2-Cp* ligands equatorial. A comparison between **1** and **17** revealed that, whereas in **1** the charges on all five tertiary carbon atoms of the Cp* ligand were negative (−0.08 to −0.11 for each or −0.48 on all five carbons), in **17** the two carbon atoms closest to iridium had a combined charge of −0.42 while the three displaced carbon atoms had a combined charge of + 0.06. Only two of the Cp* carbon atoms are bound to iridium in **17**. The energy of intermediate **17** was found to be only 3.7 kcal/mol higher than **1**. This result suggests that a large amount of reorganization energy is required in the transition state to displace the Cp* ligand. Reductive elimination of CF_3H from **17**, simultaneous with recoordination of the Cp* ring (η^2- to η^5-Cp*), was calculated to occur via **TS-3** with $\Delta G^{\ddagger}$-(298.15 K) = 41.8 kcal/mol relative to **1**. Presumably, an equal amount of reorganization energy is required to recoordinate the Cp* ligand in **TS-3** as was needed in **TS-2**. However, the loss of CF_3H in **TS-3** contributes to the lowering of the barrier for reductive elimination because of entropic effects.

We also considered the possibility of CO dissociation from intermediate **17** to give **3**. Unfortunately, attempts to locate a transition state connecting **17** and **3** were unsuccessful. Systematically increasing the Ir−(CO) bond distance in **17** and performing transition state searches either resulted in immediate recoordination of CO to iridium or loss of CO to give **3**. We believe, therefore, that if intermediate **17** were formed in the reaction, CO loss would be rapid to give **3** with a barrier much lower than that required to reach **TS-3**. Because neither intermediate **17** nor product **3** were observed experimentally, and treatment of **42** with CO did not induce R_F−H reductive elimination (eq 17, vide supra), we conclude the mechanism illustrated in path D is not kinetically feasible.

Loss of CF_3H from 1: Solution-Phase Calculations. The calculations for the loss of CF_3H from **1** were repeated to compute solvation energies and structures (Table 5 and Figure 4). In solvation calculations, structures are first optimized in the gas phase, and then the results are subjected to solvation effects, which include reoptimization of the geometries. This method utilizes the Poisson−Boltzmann continuum approximation, which represents the solvent as a layer of charges at the molecular surface using the dielectric constant and probe radius for the selected solvent.[59,60] Recent work has appeared in the literature employing this technique.[61−63] The solvation energy (E_{solv}) of a structure is defined as the (optimized gas-phase energy) − (optimized solution-phase energy). For all organometallic structures (except for **TS-1**), E_{solv} was calculated to be approximately −4 kcal/mol in benzene and −8 to −11 kcal/mol in methanol. **TS-1** was calculated to have an E_{solv} value of −12.5 kcal/mol in benzene and −30.4 kcal/mol in methanol, significantly larger than the other calculated solvation energies.

The geometries of solvated species were not significantly perturbed compared to the gas-phase optimized structures except for **TS-1** (see Table S-3 in the Supporting Information for selected bond lengths). In **TS-1**, the acyl C−CF_3 bond distance was predicted to increase from 2.884 Å in the gas-phase calculation to 3.105 Å in the benzene-solvent calculation, and to 3.484 Å in the methanol-solvent calculation. The Ir−H calculated distance in **TS-1** remained at 1.580 Å in the gas-phase and benzene-solvent calculations, but increased slightly to 1.589 Å in the methanol-solvent calculation. NBO analyses of **TS-1** revealed that a −0.88 and −0.94 charge accumulated

(58) Hughes, R. P.; Kovacik, I.; Lindner, D. C.; Smith, J. M.; Willemsen, S.; Zhang, D. H.; Guzei, I. A.; Rheingold, A. L. *Organometallics* **2001**, *20*, 3190−3197.

(59) Tannor, D. J.; Marten, B.; Murphy, R.; Friesner, R. A.; Sitkoff, D.; Nicholls, A.; Ringnalda, M.; Goddard, W. A.; Honig, B. *J. Am. Chem. Soc.* **1994**, *116*, 11875−11882.

(60) Marten, B.; Kim, K.; Cortis, C.; Friesner, R. A.; Murphy, R. B.; Ringnalda, M. N.; Sitkoff, D.; Honig, B. *J. Phys. Chem.* **1996**, *100*, 11775−11788.

(61) Oxgaard, J.; Muller, R. P.; Goddard, W. A.; Periana, R. A. *J. Am. Chem. Soc.* **2004**, *126*, 352−363.

(62) Xu, X.; Kua, J.; Periana, R. A.; Goddard, W. A. *Organometallics* **2003**, *22*, 2057−2068.

(63) Baik, M. H.; Friesner, R. A.; Lippard, S. J. *J. Am. Chem. Soc.* **2003**, *125*, 14082−14092.

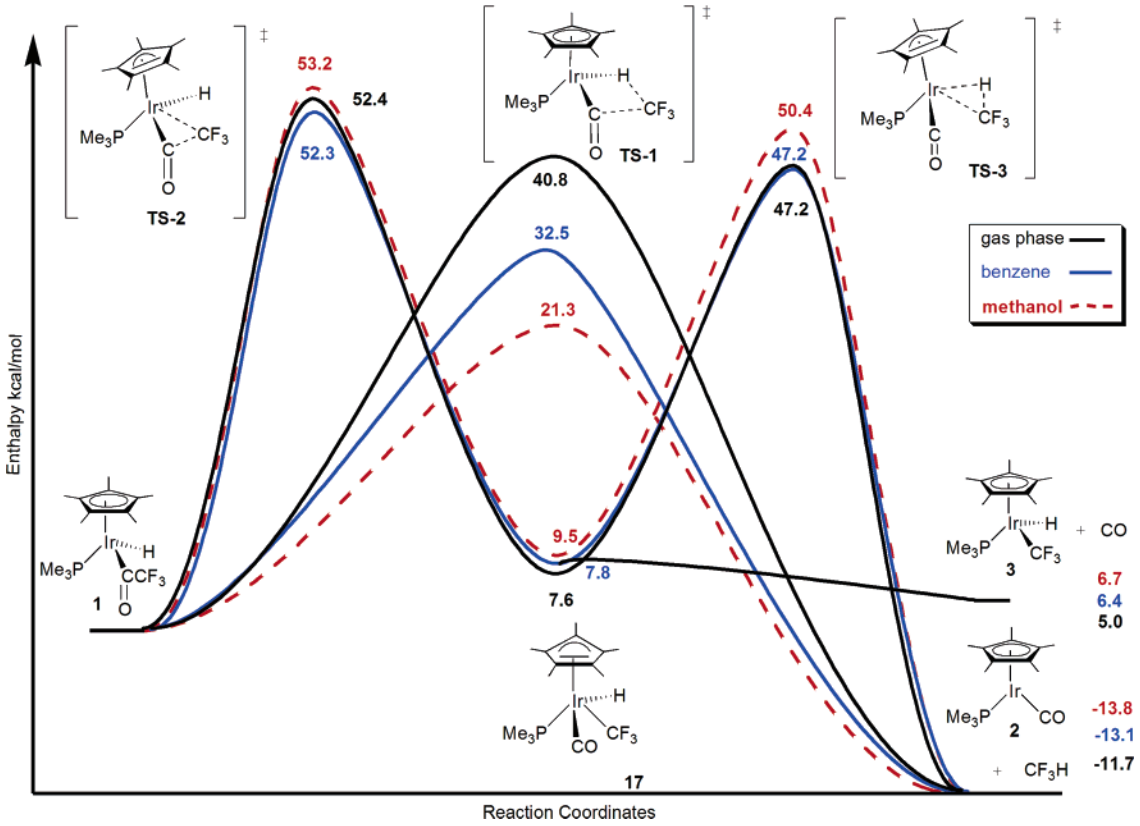

Figure 4. Energy diagram for CF_3H elimination from **1** calculated in the gas phase, benzene, and methanol. Geometries were optimized using B3LYP/LACVP**. Single-point calculations were performed at the B3LYP/LACVP**++ level of theory. ZPE and Gibbs free energy corrections are not included.

on the CF_3 fragment for the benzene and methanol-solvent calculations. No significant geometrical changes occurred for **TS-2** or **TS-3** in the solution-phase calculations.

The effects of introducing solvent into the molecular environment on the structures and energies of the calculated species were most pronounced for **TS-1** and were the result of compensating for the change in charge distribution. The large E_{solv} and the elongation of the acyl C−CF_3 bond length calculated upon going from the gas-phase to benzene and finally methanol solvent for **TS-1** are consistent with experimental observations which demonstrated that the reaction described in Scheme 1 occurs through an ion-pair mechanism. While we cannot definitely state that the structure labeled **TS-1** is truly a transition state and not an intermediate when solvent-inclusive calculations are performed, experimentally we know that this "ion pair" has a long enough lifetime for the trifluoromethyl anion to be trapped by proton donation from solvent. In addition, M−H bond-breaking must be very weakly developed in this species to account for the negligible isotope effect (vide infra).

Calculated Isotope Effect for CF_3H/D Elimination from 1. Substitution of deuterium for hydrogen at the iridium center was done to determine whether a KIE would be predicted for the loss of CF_3H from **1** (experimentally, no KIE was measured for the loss of CF_3H from **1**). The Gibbs free energies of all calculated structures decreased upon D for H substitution. For example, the calculated $\Delta\Delta G°$(**1** − **1-D**) = −1.64 kcal/mol. The calculated $\Delta\Delta G°$ caused by substituting D and H for all other compounds is given in Table 7. Using the difference in activation energy ($\Delta\Delta G^{‡}$) between the deuterated and protiated compounds, the KIE was calculated for both mechanisms

Table 7. Calculated Isotope Effect for the Elimination of CF_3H/D from **1**

compound	$\Delta G°$ of D and H for given compound (kcal/mol)	$\Delta G^{‡}$ of ground state and TS for H and D (kcal/mol)	k_H/k_D
1[a,b]			
1-D[a,b]	−1.64		
1[a,c]			
1-D[a,c]	−1.55		
17			
17-D	−1.64		
TS-1		46.02	
TS-1-D	−1.55	46.12	1.17
TS-2		50.89	
TS-2-D	−1.56	50.87	0.97
TS-3		38.17	
TS-3-D	−1.26	38.55	1.90

[a] Two rotomers for **1** were found. It was determined that one conformation led directly to **TS-1** while the other conformation led to **TS-2**. [b] Rotomer leading to **TS-1**. [c] Rotomer leading to **TS-2**.

illustrated in Figure 3. Calculations predicted a KIE of 1.17 for the concerted but highly asynchronous mechanism, 0.97 for migration of CF_3 to Ir, and 1.90 for loss of $CF_3H(D)$.

The negligible KIE of 0.97 for migration of CF_3 to iridium is expected because the metal hydride bond is not being broken. A KIE of 1.90 was calculated for the reductive elimination of CF_3H from intermediate **17**. However, because this step occurs after the rate-determining **TS-2**, the KIE would not be observed experimentally. The small calculated KIE for the concerted elimination reaction is consistent with the experiment results and re-enforces the notion that CF_3^- dissociation occurs before the Ir−H bond is broken.

Conclusions

The conversion of **1** into CF_3H and the iridium carbonyl product **2** defines a new reaction of metal acyl complexes. The following experimental observations provide strong evidence for a mechanism that invokes a metal cation/carbanion ion-pair intermediate. (1) The rate of reaction was greatly accelerated in polar aprotic solvents. (2) No KIE was observed for the elimination of CF_3H from **1**, suggesting that the Ir−H bond undergoes little bond-breaking in the rate-limiting step. (3) Isotope tracer studies revealed that, in deuterated solvents, deuterium was incorporated into the trifluoromethane product by protonolysis of CF_3^-. (4) Other acyl complexes were synthesized and found to also undergo anion dissociation. The rate at which R−H elimination occurred appears to be related to the electron-withdrawing ability of the dissociated anion and steric bulk at the acyl group. For example, complexes with longer perfluoroacyl substituents eliminated R_F−H at faster rates than **1**. (5) Additionally, whether the molecular orbitals of the acyl substituent are configurationally aligned with the acyl group in the transition state, so as to stabilize the developing carbanion, strongly influences the rate of anion dissociation. (6) Using an α-chiral acid chloride, it was shown that R−H elimination occurred with a high degree of retention of configuration. (7) β-Elimination products arising from fluoride loss were observed.

In support of the above experimental results, computational studies showed that inclusion of solvation effects was essential to predicting the barrier heights for CF_3H elimination from **1**. In gas-phase calculations, the energy of CF_3^- dissociation was found to be prohibitively high for the thermal reaction, which occurred experimentally with $t_{1/2} < 10$ min at 105 °C in methanol. However, by introducing solvent into the molecular environment, the structure of **TS-1** changed to one which more closely resembles an intermediate ion pair with a drastic decrease in energy relative to alternative transition states. An alternative mechanism involving migration of CF_3 to iridium was calculated. This mechanism was discarded because of the high reaction barriers and a low energy path that led to the incorrect products.

Experimental Section

General. All experiments were performed using standard Schlenk and vacuum line techniques or in a Vacuum Atmosphere glovebox under an inert atmosphere of N_2 unless otherwise noted. Glassware was dried at 160 °C prior to use. All reagents were used as received from commercial suppliers unless otherwise noted. THF (Fisher) was distilled from sodium/benzophenone ketyl under nitrogen and stored over 3 Å molecular sieves in the glovebox. Diethyl ether, benzene, toluene, hexane, pentane, and dichloromethane (Fisher) were passed through a column of activated alumina (type A2, size 12 × 32, Purify Co.) under nitrogen pressure, sparged with N_2, and stored over 3 Å molecular sieves in the glovebox prior to use. Deuterated solvents were purchased from Cambridge Isotope Laboratories, degassed and distilled from the proper drying agent, and stored over 3 Å sieves. *tert*-Butyllithium (Aldrich) was recrystallized multiple times from pentane at −38 °C (until white) and stored at −38 °C. Methyl iodide was stored under vacuum over copper wire. Silica gel used for chromatography was dried under vacuum at 300 °C for 2 days and stored in the glovebox.

All NMR spectra were obtained using Bruker AV-400 or DRX-500 MHz spectrometers. Unless otherwise indicated, NMR spectra were recorded at 22 °C. Chemical shifts are reported in parts per million (ppm). ^{1}H NMR spectra were recorded at 400 or 500 MHz, and chemical shifts were referenced to the residual protiated solvent peak. ^{13}C NMR spectra are proton decoupled and were recorded at 125 or at 100 MHz; chemical shifts were referenced to the solvent. ^{19}F NMR spectra were recorded at 376 MHz, and chemical shifts are reported relative to external $CFCl_3$. ^{31}P NMR spectra were recorded at 162 MHz; chemical shifts were referenced to an external standard of trimethyl phosphate. Pyrex NMR tubes equipped with resealable Teflon stopcocks were used in some procedures and are referred to as J. Young tubes.

Gases and some volatile liquids were condensed into reaction vessels at −196 °C employing known-volume bulbs and a Baratron pressure gauge. Infrared (IR) spectra were recorded using either a Mattson Instrument Galaxy 300 Fourier transformer spectrometer (for solution IR) or a Thermal Nicolet Avatar 370 FT-IR spectrometer equipped with a Smart Performer ATR (for solid IR) and are reported in wavenumbers (cm^{-1}). Elemental analyses were performed at the UC-Berkeley Microanalytical facility with a Perkin-Elmer 2400 Series II CHNO/S Analyzer. Gas chromatograph-mass spectroscopy (GC-MS) data were obtained using an Agilent Technologies Instrument 6890N GC (column #HP-5MS, 30.0 m × 250 μm × 0.25 μm calibrated) and 5973N MS. Mass spectroscopy on compound **7** was collected using a Quattro triple quadrupole instrument (Micromass) equipped with an electrospray ion source. The source was operated in positive mode, capillary voltage −4 kV, cone voltage −52 V. The sample flow rate was 10 μL/min.

Chiral gas chromatography was carried out using a HP 5890 Series II instrument equipped with a Chiraldex G-TA column. The column was pressurized at 20 psi. The oven temperature profile was as follows: initial temperature 70 °C for 25 min, ramp 5 °C/min to 120 °C, hold at 120 °C for 10 min, then cool 15 °C/min back to 70 °C. The alkene **34** was detected at 11.5 min. The alkane **33** was detected at 12.8 and 19.9 min depending on the enantiomer. The (*R*)-aldehyde **32** was detected at 35.3 min, and the (*S*)-aldehyde **32** was detected at 36.4 min. Chiral HPLC analyses were performed using a HP 1100 system with a HP 1100 Diode Array Detector (monitoring at 210, 220, 230, 254, and 280 nm) using a Daicel CHIRACEL OD column (4.6 × 250 mm) with a flow rate of 1 mL/min. Optical rotations were measured on a Perkin-Elmer model 241 polarimeter equipped with a sodium lamp.

Synthesis. The following compounds were made according to literature procedures: $Cp^*(PMe_3)Ir(H)_2$ (**4**),[64] $Cp^*(PMe_3)Ir(D)_2$,[26] $Cp^*(PMe_3)Ir(CO)$ (**2**),[65] $Cp^*(PMe_3)Ir(H)[C(O)$-*tert*-$C_4H_9]$ (**11**) and $Cp^*(PMe_3)Ir(H)[C(O)$-*p*-$NO_2C_6H_4]$ (**12**),[24] $[Cp^*(PMe_3)Ir(H)(CO)]O_3SCF_3$ (**21**),[57] $[Cp^*(PMe_3)Ir(Me)(CO)]O_3SCF_3$ (**37-OTf**),[66] $Cp^*(PMe_3)IrH(CF_2CF_2CF_3)$ (**42**),[58] 9*H*-fluorene-9-carbonyl chloride (**24**),[67] 9-methyl-9*H*-fluorene-9-carboxylic acid,[68] 2-methyl-2-phenyl-propionyl chloride,[69] cyano-dimethylacetyl chloride,[70] $[Ph_3C][B(C_6F_5)_4]$,[71] and thallium(I) *N*-hydroxypyridine-2-thione.[54] All new iridium acyl hydrides, except **5**, were synthesized on the basis of the method developed by Paisner et al.[24]

$Cp^*(PMe_3)Ir(H)[C(O)CF_3]$ (1). A resealable 250-mL Schlenk flask equipped with a stir bar and Teflon stopper was charged with $Cp^*(PMe_3)Ir(H)_2$ (401 mg, 1.00 mmol), 1,8-bis(dimethylamino)-naphthalene (257 mg, 1.20 mmol), and toluene (30 mL). The flask was connected to a vacuum manifold, and the solution was subjected to three freeze−pump−thaw cycles. At −196 °C, trifluoroacetyl chloride (1.20 mmol) was condensed into the flask. The solution was then thawed by warming to room temperature to give a yellow solution containing copious amounts of white precipitate. After the mixture was stirred for 18 h,

(64) Heinekey, D. M.; Hinkle, A. S.; Close, J. D. *J. Am. Chem. Soc.* **1996**, *118*, 5353−5361.
(65) Del Paggio, A. A.; Muetterties, E. L.; Heinekey, D. M.; Day, V. W.; Day, C. S. *Organometallics* **1986**, *5*, 575−581.
(66) Alaimo, P. J.; Arndtsen, B. A.; Bergman, R. G. *Organometallics* **2000**, *19*, 2130−2143.
(67) Robarge, M. J.; Husbands, S. M.; Kieltyka, A.; Brodbeck, R.; Thurkauf, A.; Newman, A. H. *J. Med. Chem.* **2001**, *44*, 3175−3186.
(68) Bavin, P. M. G. *Anal. Chem.* **1960**, *32*, 554−556.
(69) Campaigne, E.; Maulding, D. R. *J. Org. Chem.* **1963**, *28*, 1391.
(70) Biechler, S. S.; Taft, R. W. *J. Am. Chem. Soc.* **1957**, *79*, 4927−4935.
(71) Ihara, E.; Young, V. G.; Jordan, R. F. *J. Am. Chem. Soc.* **1998**, *120*, 8277−8278.

the volatile materials were removed under reduced pressure. The residual solid was taken up in diethyl ether and filtered through a small pad of silica gel on a medium-pore glass frit eluting with diethyl ether (ca. 35 mL). The yellow filtrate was evaporated to dryness in vacuo to give a yellow residue which was extracted with hexane until the extracts were colorless (ca. 12 mL). The combined hexane extracts were concentrated in vacuo to ca. 5 mL and then allowed to stand at −38 °C. After 1 d, yellow needlelike crystals formed. The mother liquor was removed via pipet, and the crystals were washed with cold pentane and dried under vacuum giving analytically pure material. Yield: 319 mg (64%). Additional crops could be isolated by combining the mother liquor and pentane washes, concentrating the solution in vacuo, and allowing it to stand at −38 °C for crystallization. Combined yields typically ranged from 70% to 90%. The monodeuterated compound **1-d** was synthesized from Cp*(PMe$_3$)Ir(D)$_2$ following the same procedure. ^{1}H NMR (C$_6$D$_6$): δ 1.76 (d, $^4J_{P-H}$ = 1.2 Hz, 15H, Cp*CH*$_3$), 1.12 (d, $^2J_{P-H}$ = 10.5 Hz, 9H, P*CH*$_3$), −16.45 (d, $^2J_{P-H}$ = 33.5 Hz, 1H, Ir*H*). ^{13}C{^{1}H} NMR (CD$_2$Cl$_2$): δ 211.0 (m, carbonyl), 121.0 (q, $^1J_{F-C}$ = 303 Hz, *C*F$_3$), 95.0 d, ($^2J_{C-P}$ = 1.3 Hz, *C*$_q$Me$_5$), 19.3 (d, $^1J_{C-P}$ = 39.0 Hz, P*CH*$_3$), 10.2 (s, Cp**CH*$_3$). ^{31}P{^{1}H} NMR (C$_6$D$_6$): −40.4. ^{19}F NMR (C$_6$D$_6$): −79.7. IR (CD$_2$Cl$_2$): 2113 (mb, Ir−H) and 1613 (s, CO), 1287, 1233, 1172, 1120, and 879. Anal. Calcd for C$_{15}$H$_{25}$F$_3$OPIr: C, 35.92; H, 5.03. Found: C, 36.06; H, 5.15.

Cp*(PMe$_3$)Ir(H)[C(O)CF$_2$CF$_3$] (5). Because the acid chloride was not commercially available, this compound was synthesized using the method developed by Peterson et al. from the iridate [Cp*(PMe$_3$)IrHLi]$_x$ and the acid anhydride.[26] In the glovebox, a 20-mL scintillation vial equipped with a Teflon stir bar was charged with Cp*(PMe$_3$)Ir(H)$_2$ (214 mg, 0.53 mmol), *tert*-butyllithium (56 mg, 0.74 mmol), and benzene (8 mL) and stirred for 10 min. Pentafluoropropionic anhydride (229 mg, 0.74 mmol) dissolved in 2 mL of benzene was added dropwise to the stirred solution, giving a dark brown suspension. After 2 h, the suspension was filtered through a pad of silica gel on a medium-pore fitted glass frit eluting with diethyl ether (ca. 50 mL). The resulting yellow-orange filtrate was evaporated to dryness, giving a brown oil. The oil was extracted with benzene/hexane (1:1) until colorless, and the extract was filtered through a glass fiber filter. The resulting yellow solution was evaporated to dryness under reduced pressure to give an oil. The oil was dissolved in a minimum amount of pentane and added to a column of silica gel (1.5" packed in a Pasteur pipet). The column was eluted with pentane collecting approximately 6 mL of a colorless fraction. Next, the column was eluted with pentane/diethyl ether (1:1) to collect 10 mL of a yellow fraction containing product. The volatile materials from the second fraction were removed under reduced pressure to give a yellow oil. The oil was dissolved in a minimum amount of pentane (ca. 2 mL) and allowed to stand at −38 °C for crystallization. After 2 days, small clusters of yellow microcrystals grew. The mother liquor was removed via pipet, and the crystals were washed with cold pentane (2 mL) and dried under reduced pressure. The mother liquor and pentane washes were combined, reduced to approximately 2 mL, and allowed to stand at −38 °C for two addition crops. Combined yield: 92 mg (32%). ^{1}H NMR (C$_6$D$_6$): δ 1.74 (d, $^4J_{P-H}$ = 1.2 Hz, 15H, Cp*CH*$_3$), 1.09 (d, $^2J_{P-H}$ = 10.8 Hz, 9H, P*CH*$_3$), −16.41 (d, $^2J_{P-H}$ = 32.0 Hz, 1H, Ir*H*). ^{19}F NMR (C$_6$D$_6$): δ −78.9 (s, 3F, C*F*$_3$), −113.2 (d, $^2J_{F-F}$ = 294 Hz, 1F, *CF*$_2$), −115.0 (d, $^2J_{F-F}$ = 294 Hz, 1F, *CF*$_2$). ^{31}P{^{1}H} NMR (C$_6$D$_6$): −40.3. IR (Solid ATR): 2128 (br, Ir−H), 1602 (s, C═O), 1211 (s), 1156 (s), 955 (s), 807 (s), 723 (s). FAB HRMS: *m*/*z* calcd for C$_{16}$H$_{24}$F$_5$OPIr 551.112589 [M]$^+$, found 551.111437.

Cp*(PMe$_3$)Ir(H)[C(O)CF$_2$CF$_2$CF$_3$] (6). In the glovebox, a 20-mL scintillation vial equipped with a Teflon stir bar was charged with Cp*(PMe$_3$)Ir(H)$_2$ (211 mg, 0.52 mmol), 1,8-bis(dimethylamino)-naphthalene (139 mg, 0.63 mmol), and benzene (10 mL). To the stirred solution, heptafluorobutyryl chloride (146 mg, 0.63 mmol) was added, producing a yellow solution with copious amounts of white precipitate. After being stirred for 18 h at room temperature, the solution was filtered though a small pad of silica gel on a medium-pore glass frit eluting with diethyl ether. The yellow filtrate was evaporated to dryness under reduced pressure to give a yellow residue which was extracted with hexane until the extracts were colorless. The hexane extracts were filtered through a glass fiber filter, and the volatile materials were evaporated under reduced pressure. The resulting oil, contaminated with starting material, was dissolved in a minimum amount of pentane and added to a column of silica gel (1.5" packed in a Pasteur pipet). First, the column was eluted with pentane (ca. 20 mL) to collect a faint yellow fraction containing unreacted proton sponge. Second, the column was eluted with diethyl ether (10 mL) to collect a yellow fraction containing product. The volatile materials from the yellow fraction were removed under reduced pressure. The resulting oil was dissolved in pentane and allowed to stand at −38 °C. After 2 days, small crystals grew. The mother liquor was removed by pipet, the crystals were washed with cold pentane, and the excess solvent was removed under reduced pressure to give 35 mg of analytically pure material. The mother liquor and pentane washes were combined, concentrated, and allowed to stand at −38 °C to obtain additional crops. Combined yield: 100 mg (32%). ^{1}H NMR (C$_6$D$_6$): δ 1.73 (d, $^4J_{P-H}$ = 1.2 Hz, 15H, Cp*CH*$_3$), 1.10 (d, $^2J_{P-H}$ = 10.4 Hz, 9H, P*CH*$_3$), −16.45 (d, $^2J_{P-H}$ = 33.6 Hz, 1H, Ir*H*). ^{19}F NMR (C$_6$D$_6$): δ −79.9 (t, $^3J_{F-F}$ = 11.3 Hz, 3F, C*F*$_3$), −109.6 (d, $^2J_{F-F}$ = 290 Hz, 1F, −*CF*$_2$−), −111.4 (d, $^2J_{F-F}$ = 297 Hz, 1F, −*CF*$_2$−), −124.7 (q, $^3J_{F-F}$ = 5.6 Hz, 2F, −*CF*$_2$−). ^{31}P{^{1}H} NMR (C$_6$D$_6$): −40.3. IR (Solid ATR): 2112 (br, Ir−H), 1608 (s, C═O). Anal. Calcd for C$_{17}$H$_{25}$F$_7$OPIr: C, 33.94; H, 4.19. Found: C, 34.18; H, 4.26.

Cp*(PMe$_3$)Ir(H)[C(O)(CF$_2$)$_7$CF$_3$] (7). The reaction was set up as described for the synthesis of **6** using Cp*(PMe$_3$)Ir(H)$_2$ (122 mg, 0.30 mmol), 1,8-bis(dimethylamino)-naphthalene (77.0 mg, 0.36 mmol), and perfluorononanoyl chloride (174 mg, 0.36 mmol). After being stirred for 18 h at room temperature, the solution was filtered though a small pad of silica gel on a medium-pore glass frit eluting with diethyl ether. The resulting solution was evaporated in vacuo to afford a yellow oil. The oil was dissolved in pentane (1 mL) and added to a column of silica gel (2" packed in a Pasteur pipet). Unreacted starting material was eluted from the column with pentane (ca. 35 mL, flash chromatography) to give a colorless fraction. The column was then flushed with diethyl ether to collect a yellow fraction containing **7**. This fraction was evaporated under reduced pressure to afford a yellow oil (yield: 127 mg, 50%) of >95% purity by NMR spectroscopy. This oil could be crystallized from a minimum amount of pentane at −38 °C to provide analytically pure material. ^{1}H NMR (C$_6$D$_6$): δ 1.74 (dd, $^4J_{P-H}$ = 1.8 Hz, $^4J_{H-H}$ 0.6, 15H, Cp**CH*$_3$), 1.11 (d, $^2J_{P-H}$ = 10.5 Hz, 9H, P*CH*$_3$), −16.46 (d, $^2J_{P-H}$ = 33.1 Hz, 1H Ir*H*). ^{31}P{^{1}H} NMR (C$_6$D$_6$): −40.4. ^{19}F NMR (C$_6$D$_6$): δ − 80.90 (t, J = 9.7 Hz), −110.0 (four lines, each split into a triplet, J = 13.5 Hz), −120.2 (s), −120.4 (s), −121.6 (m) −122.6 (s), −126.1 (s). IR (CH$_2$Cl$_2$): 3055, 2985, 2911, 2118 (mb, Ir−H), 1612 (s, CO), 1422, 1242, 715. Anal. Calcd for C$_{22}$H$_{25}$F$_{17}$OPIr: C, 31.03; H, 2.96. Found: C, 31.33; H, 2.85.

Cp*(PMe$_3$)Ir(H)[C(O)C(CH$_3$)$_2$(C$_6$H$_5$)] (8). The reaction was set up as described for the synthesis of **6** using Cp*(PMe$_3$)Ir(H)$_2$ (122 mg, 0.30 mmol), 1,8-bis(dimethylamino)naphthalene (77.0 mg, 0.36 mmol), and 2-methyl-2-phenyl-propionyl chloride (72 mg, 0.45 mmol). After the solution was stirred for 18 h, it was filtered through a medium-pore glass frit, and the volatile materials were removed under reduced pressure. The resulting orange solid was extracted with pentane (3 × 4 mL), and the pentane extracts were filtered through a glass fiber filter. The yellow filtrate was concentrated in vacuo to ca. 5 mL and allowed to stand at −38 °C overnight to afford pale yellow crystals. After the mother liquor was removed via pipet, the crystals were recrystallized from pentane at −38 °C to obtain analytically pure material. Yield: 75 mg (47%). ^{1}H NMR (C$_6$D$_6$): δ 7.52 (dt, $^3J_{H-H}$ = 8.5 Hz, $^4J_{H-H}$ = 1.5 Hz, 2H, *aryl*), 7.19 (tt, $^3J_{H-H}$ = 8.5 Hz, $^4J_{H-H}$ = 5.5 Hz, 2H, *aryl*), 7.07 (tt, $^3J_{H-H}$ = 7.3 Hz, $^4J_{H-H}$ = 1.2 Hz, 1H, *aryl*), 1.83 (s, 3H, benzyl*CH*$_3$), 1.78 (dd, $^4J_{P-H}$ = 1.8 Hz, $^4J_{H-H}$ = 0.6 Hz 15H, Cp*CH*$_3$), 1.76 (s, 3H, benzyl*CH*$_3$), 0.88 (d, $^2J_{P-H}$ = 10.4 Hz, 9H, P*CH*$_3$), −16.79 (d, $^2J_{P-H}$ = 35.4 Hz, 1H, Ir*H*). ^{13}C{^{1}H} NMR (C$_6$D$_6$): δ 228.5, 146.1,

128.5, 127.8, 125.4, 94.1, 53.9, 29.8, 29.3, 18.8 (d, J_{C-P} = 37.9 Hz, P*CH*$_3$), 10.7. ^{31}P{^{1}H} (C_6D_6): δ −40.6. IR (pentane): 2111 (mb, Ir−H), 1588 (s, CO), 1281, 955, 855, and 899. Anal. Calcd for $C_{23}H_{36}$OPIr: C, 50.07; H, 6.58 Found: C, 50.18; H, 6.54.

Cp*(PMe$_3$)Ir(H)[C(O)C(CH$_3$)$_2$(CO$_2$CH$_3$)] (9). The reaction was set up as described for the synthesis of **6** using Cp*(PMe$_3$)Ir(H)$_2$ (122 mg, 0.30 mmol), 1,8-bis(dimethylamino)naphthalene (77.0 mg, 0.36 mmol), 2-chlorocarbonyl-2-methylpropionic acid methyl ester (59.0 mg, 0.36 mmol), and toluene (10 mL). After 2 days, the reaction was worked up as described for the synthesis of **8** to afford white microcrystals. Yield: 78 mg (49%). An additional crop could be isolated from the mother liquor after concentrating it in vacuo and allowing it to stand at −38 °C. Crop 2 yield: 28 mg (18%). ^{1}H NMR (C_6D_6): δ 1.98 (s, 3H, O*CH*$_3$), 1.80 (m, 18H, propyl*CH*$_3$ and Cp*CH*$_3$), 1.70 (s, 3H, propyl*CH*$_3$), 1.29 (d, $^2J_{P-H}$ = 10.5 Hz, 9H, P*CH*$_3$), −17.12 (d, $^2J_{P-H}$ = 32.4 Hz, 1H, Ir*H*). ^{13}C{^{1}H} NMR (C_6D_6): δ 219.9, 169.5, 98.1, 94.5, 25.6, 25.0, 22.4, 19.6 (d, $^1J_{C-P}$ = 38.0 Hz, P*CH*$_3$), 11.6. ^{31}P{^{1}H} (C_6D_6): δ −42.0. IR (pentane): 2151 (br, Ir−H), 1738 and 1607 (two C═O), 1290, 1148, 956, 879, and 729. Anal. Calcd for $C_{19}H_{34}O_3$PIr: C, 42.76; H, 6.24 Found: C, 42.95; H, 6.07.

Cp*(PMe$_3$)Ir(H)[C(O)C(CH$_3$)$_2$(CN)] (10). The reaction was set up as described for the synthesis of **6** using Cp*(PMe$_3$)Ir(H)$_2$ (142 mg, 0.35 mmol), 1,8-bis(dimethylamino)naphthalene (77.0 mg, 0.36 mmol), cyano-dimethyl-acetyl chloride (59.0 mg, 0.45 mmol), and toluene (10 mL). After 4 h, the reaction was worked up as described for the synthesis of **8** to afford yellow cubic microcrystals. Yield: 78 mg (49%). An additional crop could be isolated from the mother liquor after concentrating it in vacuo and allowing it to stand at −38 °C. Crop 2 yield: 28 mg (18%). ^{1}H NMR (C_6D_6): δ 1.80 (s, 15H, Cp*CH*$_3$), 1.32 (s, 3H, *CH*$_3$), 1.30 (s, 3H, *CH*$_3$), 1.19 (d, $^2J_{P-H}$ = 10.4 Hz, 9H, P*CH*$_3$), −16.25 (d, $^2J_{P-H}$ = 33.6 Hz, 1H, Ir*H*). ^{13}C{^{1}H} NMR (C_6D_6): δ 216.2 (m, carbonyl), 127.4, 94.6, 25.2, 24.7, 19.4 (d, $^1J_{C-P}$ = 37.1 Hz, P*CH*$_3$), 10.5 (one signal, presumably for the cyano carbon, was not located). ^{31}P{^{1}H} (C_6D_6): δ −40.6. IR (Solid ATR): 2974, 2909, 2225 (sm, C−N), 2095 (br, Ir−H), 1589 (s, C═O), 960, 942, 857, 776, and 733. Anal. Calcd for $C_{18}H_{31}$NOPIr: C, 43.18; H, 6.24; N, 2.80. Found: C, 43.05; H, 6.36; N, 3.14.

Cp*(PMe$_3$)Ir(CH$_3$)[C(O)CF$_3$] (13). A 250-mL thick-walled, resealable flask equipped with a stir bar was charged with Cp*(PMe$_3$)Ir(H)[C(O)CF$_3$] (**1**) (155 mg, 0.308 mmol) and *tert*-butyllithium (25.7 mg, 0.401 mmol). The flask was attached to a vacuum manifold and cooled to −196 °C. THF (20 mL) was vacuum transferred into the flask. The frozen reaction mixture was warmed to −15 °C over 45 min and stirred at this temperature for 10 min. The resulting orange solution was cooled to −196 °C, and MeI (0.43 mmol) was condensed into the flask. The reaction mixture was allowed to warm to −78 °C and stirred. After 20 min, the mixture was warmed to 25 °C to produce a pale yellow solution. After the mixture was stirred at 25 °C for 30 min, the volatile materials were removed in vacuo. The crude material was extracted with diethyl ether (2 mL) and filtered through a pad of silica gel on a medium-pore glass frit eluting with diethyl ether (ca. 8 mL). The resulting red-orange solution was evaporated in vacuo to dryness. The residual solid was dissolved in 2 mL of diethyl ether, layered with pentane, and allowed to stand at −38 °C. After 18 h, analytically pure, red microcrystals were collected and washed with pentane, and the excess solvent was removed under reduced pressure. Yield: 114 mg (72%). An additional crop was isolated from the mother liquor by concentrating the solution in vacuo and cooling it to −38 °C for crystallization. Crop 2 yield: 21 mg (12%). ^{1}H NMR (CD_2Cl_2): δ 1.73 (d, $^4J_{P-H}$ = 1.5 Hz, 15H, Cp−*CH*$_3$), 1.42 (d, $^2J_{P-H}$ = 10.5 Hz, 9H, P−*CH*$_3$), 0.36 (d, $^3J_{P-H}$ = 6.0 Hz, 3H, Ir*CH*$_3$). ^{13}C{^{1}H} NMR (CD_2Cl_2): δ 225.0 (m, carbonyl*C*$_q$), 121.7 (dq $^3J_{P-C}$ = 2.1 Hz, $^2J_{F-C}$ = 302 Hz, acyl*CF*$_3$), 95.8 (d, $^2J_{C-P}$ = 2.8 Hz, *C*$_q$Me$_5$), 15.0 (d, $^1J_{C-P}$ = 38.9 Hz, P*CH*$_3$), 9.2 (s, Cp**CH*$_3$), −24.7 (d, $^2J_{C-P}$ = 6.3 Hz, Ir*CH*$_3$). ^{31}P{^{1}H} NMR (CD_2Cl_2): −35.3. ^{19}F NMR (CD_2Cl_2): −76.5. IR (pentane): 1619 (s, C═O), 1284, 1233, 1173, 1125, 956, 877, 723, 678. Anal. Calcd for $C_{15}H_{24}ClF_3OPIr$: C, 37.22; H, 5.28. Found: C, 36.97; H, 5.49.

Cp*(PMe$_3$)Ir(Cl)[C(O)CF$_3$] (14). The reaction was set up as described for the synthesis of **1** using Cp*(PMe$_3$)Ir(H)$_2$ (201 mg, 0.50 mmol), 1,8-bis(dimethylamino)naphthalene (129 mg, 0.50 mmol), hexane (15 mL), and excess trifluoroacetyl chloride (6.50 mmol). After the suspension was stirred for 18 h at room temperature, the volatile materials were removed under reduced pressure. The resulting yellow-orange solid was dissolved in CH_2Cl_2 and filtered through a pad of silica gel on a medium-pore glass frit. The yellow filtrate was concentrated in vacuo to approximately 3 mL, layered with pentane, and allowed to stand at −38 °C. After 24 h, reddish-yellow blocklike crystals grew. The mother liquor was removed via pipet, and the excess solvent was removed under reduced pressure to give analytically pure material. Yield: 158 mg (59% yield). Additional crops could be isolated by concentrating the mother liquor in vacuo, layering with pentane, and cooling to −38 °C. Combined yields were typically about 85%. ^{1}H NMR (CD_2Cl_2): δ 1.68 (d, $^4J_{P-H}$ = 2.0 Hz, 15H, Cp**CH*$_3$), 1.53 (d, $^2J_{P-H}$ = 11.5 Hz, 9H, P*CH*$_3$). ^{13}C {^{1}H} NMR (CD_2Cl_2): δ 216.3 (dq, $^2J_{P-C}$ = 16 Hz, $^2J_{F-C}$ = 31, carbonyl*C*), 122.0 (dq $^3J_{P-C}$ = 4 Hz, $^2J_{F-C}$ = 305 Hz, acyl*CF*$_3$), 95.4 (d, $^2J_{C-P}$ = 2.6 Hz, *C*$_q$Me$_5$), 13.9 (d, $^1J_{C-P}$ = 39.5 Hz, P−*CH*$_3$), 8.8 (s, Cp**CH*$_3$). ^{31}P{^{1}H} NMR (CD_2Cl_2): −27.9. ^{19}F NMR (CD_2Cl_2): −75.5. IR (CH_2Cl_2): 2980, 2917, 1630 (s, C═O), 1285, 1232, 1177, 1129, 958, 874. Anal. Calcd for $C_{15}H_{24}ClF_3$-OPIr: C, 33.61; H, 4.51. Found: C, 33.76; H, 4.39.

[Cp*(PMe$_3$)Ir(CO)(CF$_3$)][B(C$_6$F$_5$)$_4$] (23). In a 20-mL scintillation vial equipped with a stir bar, **1** (99 mg, 0.197 mmol) and [Ph$_3$C][B(C$_6$F$_5$)$_4$] (182 mg, 0.197 mmol) were added followed by toluene (10 mL). After the yellow suspension was stirred for 18 h, pentane (5 mL) was added and the suspension was allowed to settle. The mother liquor was removed by pipet, and the yellow solid was washed with pentane (3 × 5 mL). The solid was dissolved in CH_2Cl_2, layered with pentane, and put at −38 °C for crystallization. After 1 day, brown crystals grew. The mother liquor was removed by pipet, the crystals were washed with cold CH_2Cl_2 (2 mL), and the excess solvent was removed under reduced pressure. Yield: 49 mg, 21.1%. The mother liquor and CH_2Cl_2 washes were combined, concentrated, and put at −38 °C for a second crop of faint yellow crystals. Yield: 76 mg, 32.7%. A third crop was obtained upon further concentration of the mother liquor (yield: 18 mg, 7.9%). All three crops were equally pure by NMR analysis; however, crop 2 was used for elemental analysis. ^{1}H NMR (CD_2Cl_2): δ 2.10 (d, $^4J_{P-H}$ = 2.0 Hz, 15H, Cp**CH*$_3$), 1.83 (d, $^2J_{P-H}$ = 11.6 Hz, 9H, P*CH*$_3$). ^{13}C{^{1}H} NMR (CD_2Cl_2): δ 163.22 (s, carbonyl), 105.6 (s, *C*$_q$Me$_5$), 16.7 (d, $^1J_{C-P}$ = 41.3 Hz, P−*CH*$_3$), 9.3 (s, Cp**CH*$_3$) (resonances for the trifluoromethyl-bound iridium and borate counterion were not resolved in the ^{13}C NMR). ^{19}F NMR (CD_2Cl_2): −5.7 (s, 3F, Ir(*CF*$_3$)), −133.0 (s, 8F, C$_{aryl}$*F*), −163.5 (s, 4F, C$_{aryl}$*F*), −167.4 (s, 8F, C$_{aryl}$*F*). ^{31}P{^{1}H} NMR (CD_2Cl_2): −37.8 (q, $^3J_{P-F}$ = 5.4 Hz). IR (CH_2Cl_2): 2065 (s, C═O), 1643, 1513, 1465, 1084, 980. Anal. Calcd for $C_{39}H_{24}BF_{23}$OPIr: C, 39.71; H, 2.05. Found: C, 39.90; H, 1.85.

3,3,3-Trifluoro-2-methoxy-2-phenylpropionaldehyde (32). Treatment of (*S*)-Mosher's acid chloride (15.6 mg, 0.062 mmol) with *n*-Bu$_3$SnH (24 mg, 0.74 mmol) in C_6D_6 (0.5 mL) afforded aldehyde **32** in 98% yield based on NMR and GC analysis after 3 days at 25 °C. The volatile materials were vacuum transferred away from tin compounds to give a solution of **32** in C_6D_6. Analysis of the product by chiral GC showed that the aldehyde was generated in >98% ee. ^{1}H NMR (C_6D_6): δ 9.27 (q, $^4J_{H-F}$ = 2.6 Hz, 1H, C(O)*H*), 7.35 (m, 2H, aryl), 6.00 (m, 3H, aryl), 3.05 (s, 3H, O*CH*$_3$). ^{19}F NMR (C_6D_6): δ −71.1 (s, 3F, *CF*$_3$).

(±)-2,2,2-Trifluoro-1-methoxyethylbenzene (33). This compound was originally synthesized enatiomerically enriched by Mosher et al. in a study to assign the absolute stereochemistry.[72] The procedure reported here was developed to synthesize racemic **33**. In a J-Young NMR tube, **35** (12.5 mg, 0.036 mmol) and *n*-Bu$_3$SnH (130 mg, 0.45

mmol) were dissolved in C_6D_6 (0.6 mL). The solution was heated at 75 °C for 3 days to give **33** in 98% yield by NMR with no other fluorine-containing products. The volatile materials were vacuum transferred to give a solution of **33** in C_6D_6 contaminated with alkyl tin products. The product was racemic as determined by chiral GC. ^{1}H NMR (C_6D_6): δ 7.25 (m, 2H, aryl), 7.06 (m, 3H, aryl), 4.07 (q, $^3J_{H-F}$ = 6.8 Hz, 1H, C*H*), 2.91 (s, 3H, OCH_3). ^{19}F NMR (C_6D_6): δ −76.3 (d, $^3J_{F-H}$ = 4 Hz, 3F, CF_3).

2-(2,2,2-Trifluoro-1-methoxy-1-phenyl-ethylsulfanyl)-pyridine (35). In a 20-mL scintillation vial equipped with a stir bar, thallium(I) *N*-hydroxypyridine-2-thione (318 mg, 0.96 mmol)[54] and (*R*)-Mosher's acid chloride (243 mg, 0.96 mmol) were mixed as a suspension in 18 mL of diethyl ether. The suspension was stirred for 14 h, and then filtered through a medium-pore fitted glass frit eluting with diethyl ether (20 mL). The resulting yellow solution was concentrated in vacuo under reduced pressure to give an oil. Diethyl ether (5 mL) was added to the oil and then removed under reduced pressure. After this process was repeated three times, the oil began to solidify. The crude material was dissolved in a minimum amount of diethyl ether and put at −38 °C. After 2 days, large colorless cubic-like crystals formed. The mother liquor was removed by pipet, and the crystals were recrystallized from diethyl ether at −38 °C. Yield: 103 mg (36%). An additional crop was grown from the combined mother liquors after concentrating the solution under reduced pressure and allowing it to stand at −38 °C. Optical rotation for crystals $[\alpha]^{23}_D = 0.00$ (c = 1.2, in $CHCl_3$). Chiral HPLC of isolated crystals detected **35** as a 1:1 ratio of enantiomers at 5.61 and 6.41 min (hexanes:isoproponal 95:5). The mother liquor was also analyzed by chiral HPLC. The two enantiomers were detected with ca. 9% ee. ^{1}H NMR (CD_3CN): δ 8.45 (ddd, J = 5, 2, 1 Hz, 1H), 7.70 (m, 2H), 7.62 (dt, J = 8, 2 Hz, 1H), 7.50 (d, J = 8 Hz, 1H), 7.42 (m, J = 5, 2 Hz, 3H), 7.22 (ddd, J = 8, 5, 1 Hz, 1H), 3.73 (s, 3H, OCH_3). ^{19}F NMR (CD_3CN): δ −74.7 (s, 3F, CF_3). ^{13}C{^{1}H} NMR (CD_3CN): δ 154.6, 150.8, 138.1, 134.9, 130.8, 129.5, 129.4, 129.3, 128.4, 126.2, 123.9, 121.6, 94.4 (q, J_{C-F} = 29.3 Hz), 54.2. IR (Solid ATR): 2978.2 (w), 2943.8 (w), 1573.5 (m), 1561.5 (m), 1448.6 (m), 1418.2 (m), 1268.7 (m), 1177.6 (s), 1168.6 (s), 1149.5 (s), 1093.2 (m), 1079.1 (m), 972.9 (m), 878.9 (s), 772.7 (m), 762.8 (s), 720.5 (s), 700.2 (m), 600.0 (m). Anal. Calcd for $C_{14}H_{12}F_3O_1NS$: C, 56.18; H, 4.04; N, 4.68. Found: C, 56.15; H, 4.08; N, 4.94. EI/MS: [M^+] = 299. FAB/MS: [M + 1] = 300.

Elimination of CF_3 from 14. Upon heating **14** (7 mg, 0.013 mmol) in CD_3OD (0.5 mL) at 105 °C for 6 days, the expected carbonyl chloride cation $[Cp^*(PMe_3)Ir(Cl)(CO)]^+$ was not observed via NMR spectroscopy. Instead, $[Cp^*(PMe_3)Ir(CO)(D)]^+Cl$ was identified by NMR and IR spectroscopy. The identity of this carbonyl cation was confirmed by repeating the reaction in CH_3OH and comparing the ^{1}H and ^{31}P NMR spectra of the product in DMSO-d_6, and the IR spectrum in CH_2Cl_2, to those of an authentic sample of $[Cp^*(PMe_3)Ir(CO)(H)]^+[O_3SCF_3]$, which was synthesized by the method of Angelici and co-workers.[57]

Kinetics. Rate constants were measured by NMR spectroscopy. Samples were prepared in NMR tubes, which were then sealed under vacuum. For first-order reactions, concentrations of approximately 0.02 M were used for starting material and the internal standard 1,3,5-trimethoxybenzene.[73] For trapping experiments with **13** and added **37-OTF** (OTf = $O_3S(CF_3)$ as the anion) and acid, concentrations were determined by the weight of added reagents and checked by NMR integration. NMR tubes were either heated in a constant temperature oil bath or in the probe of the NMR spectrometer. Ethylene glycol (100%) in a sealed NMR tube was used to calibrate the temperature of the probe. Reactions were monitored to at least 95% completion using one-pulse ^{1}H NMR spectroscopy at specified time intervals. The starting material and product concentrations were monitored versus the internal standard and fit to a single-exponential decay or growth function. For **1**, the data obtained by monitoring the decay of the Cp* or PMe_3 resonances had less scatter in the exponential fit than the fits for the data obtained by monitoring the decay of the iridium hydride resonance. (Presumably, this error is due to a decreasing signal-to-noise ratio for the smaller, upfield hydride resonance over the course of the reaction.) The reported rate constants are, therefore, those measured using the Cp* and PMe_3 signals. Usually, the rate constants calculated for the first-order decay and first-order growth processes were in very good agreement, which is indicative of the absence of side reactions. Exceptions occurred in a few reactions carried out in CD_3OD in which the product Cp* ligand suffered from H/D exchange with the solvent; in those cases, the product growth could not be monitored via Cp* appearance. The starting Cp* resonance of **1** in CD_3CN overlapped with the residual solvent peak; therefore, the rate constant was determined by monitoring the PMe_3 methyl resonance. Rate constants reported for the thermal reaction of **14** in C_6D_6 and DMSO-d_6 were obtained by monitoring the disappearance of starting material because no identifiable product was generated over the course of the reaction. Rate constants measured from trapping experiments with **13** and added acid were obtained by monitoring the disappearance of starting material.

Computational Details

Method. Quantum mechanical calculations were performed at the University of California, Berkeley Molecular Graphics Facility using a 98 cpu-cluster with 2.8 GHz Xeon processors. DFT calculations were carried out by implementing the B3LYP exchange-correlation functional[74−76] with the LACVP** basis set using Jaguar 5.0 or 5.5.[77] This method replaces the innermost 60 electrons of iridium with a nonlocal effect core potential (ECP).[78] All other atoms are described by the 6-31G** basis set (valence double-ζ plus polarization) developed by Pople and co-workers.[79] Geometries were fully optimized in the gas phase using the LACVP** basis set followed by single-point calculations using the LACVP**++ basis set, which places polarization functions and diffuse orbitals on all atoms except iridium. NBO analyses were calculated during the single-point calculations.[80] Vibrational frequencies were calculated to ensure that local minima lacked any negative frequencies and to confirm that transition states had only one imaginary (negative) frequency. Occasionally, "soft" vibrations (<10 cm^{-1}) were found during frequency calculations that were not included in the zero-point energy. Visual inspection of these vibrations using the Molden software program[81] revealed that they were small "wags" or "twists", usually in a methyl group, and, hence, determined to be artifacts of negligible significance to the overall energy, structure, or location along the reaction coordinate surface. Quick pseudospectral calculations developed by Jaguar were used for most calculations. However, **TS-1** and **3** did not converge using the standard method. For these calculations, fully analytical numerical methods were required, and the accuracy of the SCF grids was set to ultrafine (nops=1 and iacc=1 added to input). The magnitude of the pseudospectral error was estimated to be <0.5 kcal/mol by comparing the energies of **1** and **2** calculated at both the standard method and the fully analytical method.

Vibrational frequency analyses were not performed on solvent-inclusive calculations. Ground states and transition states were confirmed by vibrational frequency analyses for gas-phase calculations. These optimized structures were then used in solvation calculations.

(72) Peters, H. M.; Feigl, D. M.; Mosher, H. S. *J. Org. Chem.* **1968**, *33*, 4245−4250.
(73) Higher sample concentrations did not affect the observed rates of reactions.
(74) Vosko, S. H.; Wilk, L.; Nusair, M. *Can. J. Phys.* **1980**, *58*, 1200−1211.
(75) Becke, A. D. *J. Chem. Phys.* **1993**, *98*, 5648−5652.
(76) Lee, C. T.; Yang, W. T.; Parr, R. G. *Phys. Rev. B* **1988**, *37*, 785−789.
(77) *Jaguar 5.0*; Schrödinger LLC: Portland, OR, 2002.
(78) Hay, P. J.; Wadt, W. R. *J. Chem. Phys.* **1985**, *82*, 299−310.
(79) Krishnan, R.; Binkley, J. S.; Seeger, R.; Pople, J. A. *J. Chem. Phys.* **1980**, *72*, 650−654.
(80) *NBO, 5.0*; Theoretical Chemistry Institute, University of Wisconsin, Madison: Madison, WI, 2001.
(81) Schaftenaar, G.; Noordik, J. H. *J. Comput.-Aided Mol. Des.* **2000**, *14*, 123−134.

The Gibb's free energies could not be assessed due to this limitation. Therefore, energies for solvation calculations are discussed only with respect to enthalpy at 0 K relative to **1**.

To calculate kinetic isotope effects, frequency calculations were repeated in which hydrogen was replaced with deuterium. All calculations to determine the KIE of CF_3H/D elimination from **1** were done using Jaguar 5.5 and the fully analytical method with an ultrafine SCF grid to prevent the occurrence of systematic errors.

Acknowledgment. We thank Dr. Forrest Michael, Dr. Jennifer Krumper, and Ms. Cathleen M. Yung for helpful discussions. We also thank Mr. Ian C. Stuart and Ms. Rebecca M. Wilson for help with acquiring HPLC data. Funding was provided by the National Science Foundation (Grant No. CHE-0094349). We are also grateful for an equipment grant from the NSF (Grant No. CHE-0233882) for the computational facilities.

Supporting Information Available: Chart for compound numbering. Atom labeling scheme of **1**. Molecular representations of calculated species of all structures described in Figure 3. Cartesian coordinates, bond lengths, and results of vibrational frequency analyses of all compounds. This material is available free of charge via the Internet at http://pubs.acs.org.

JA045859L